



Tectonics of complex crater formation as revealed by the Haughton impact structure, Devon Island, Canadian High Arctic

Gordon R. OSINSKI^{1, 2†*} and John G. SPRAY²

¹Lunar and Planetary Laboratory, University of Arizona, 1629 East University Boulevard, Tucson, Arizona 85721–0092, USA

²Planetary and Space Science Centre, Department of Geology, University of New Brunswick,
2 Bailey Drive, Fredericton, New Brunswick E3B 5A3, Canada

[†]Present address: Canadian Space Agency, 6767 Route de l'Aéroport, Saint-Hubert, Quebec, J3Y 8Y9, Canada

*Corresponding author. E-mail: osinski@lycos.com

(Received 01 June 2004; revision accepted 19 May 2005)

Abstract—The results of a systematic field mapping campaign at the Haughton impact structure have revealed new information about the tectonic evolution of mid-size complex impact structures. These studies reveal that several structures are generated during the initial compressive outward-directed growth of the transient cavity during the excavation stage of crater formation: (1) sub-vertical radial faults and fractures; (2) sub-horizontal bedding parallel detachment faults; and (3) minor concentric faults and fractures. Uplift of the transient cavity floor toward the end of the excavation stage produces a central uplift. Compressional inward-directed deformation results in the duplication of strata along thrust faults and folds. It is notable that Haughton lacks a central topographic peak or peak ring. The gravitational collapse of transient cavity walls involves the complex interaction of a series of interconnected radial and concentric faults. While the outermost concentric faults dip in toward the crater center, the majority of the innermost faults at Haughton dip away from the center. Complex interactions between an outward-directed collapsing central uplift and inward collapsing crater walls during the final stages of crater modification resulted in a structural ring of uplifted, intensely faulted (sub-) vertical and/or overturned strata at a radial distance from the crater center of ~5.0–6.5 km. Converging flow during the collapse of transient cavity walls was accommodated by the formation of several structures: (1) sub-vertical radial faults and folds; (2) positive flower structures and chaotically brecciated ridges; (3) rollover anticlines in the hanging-walls of major listric faults; and (4) antithetic faults and crestal collapse grabens. Oblique strike-slip (i.e., centripetal) movement along concentric faults also accommodated strain during the final stages of readjustment during the crater modification stage. It is clear that deformation during collapse of the transient cavity walls at Haughton was brittle and localized along discrete fault planes separating kilometer-size blocks.

INTRODUCTION

Hypervelocity impact craters are one of the most common geological landforms in the solar system. When observing planetary bodies, such as the Moon, a striking aspect is the strong dependence of final crater morphology on crater diameter. The smallest impact craters are bowl-shaped and are referred to as “simple craters” (Dence 1964). Larger, so-called “complex impact craters,” are characterized by a structurally complicated rim, a down-faulted annular trough, and an uplifted central area, which initially takes the form of a central peak or series of peaks (Dence 1964, 1968). With increasing diameter, the central peak is accompanied by a

fragmentary ring (a central-peak basin structure), while at still larger diameters the central peak is missing and is replaced by a peak ring (peak-ring basin structure) (Grieve et al. 1981).

It is generally accepted that the final morphology of impact craters is the result of processes acting during the later stages of the impact process. That is, the modification or gravitational collapse of a bowl-shaped transient cavity (e.g., Melosh and Ivanov 1999). The effects of the modification stage are governed by the size of the transient cavity and the properties of the target (Melosh and Ivanov 1999). There are two competing mechanisms at work during crater modification. Uplift of the transient cavity floor occurs

leading to the development of a central uplift, which results in an inward and upward movement of material within the transient cavity. Concomitantly, the initially steep walls of the transient cavity collapse under gravitational forces. This induces an inward and downward movement of large (~100 m to km scale) fault-bounded blocks. Despite the importance of the modification stage in determining final crater morphology, the kinematics and mechanics of this collapse and concomitant uplift are not fully understood at present.

Numerical models are now reaching a level of complexity and realism such that they can offer important constraints on crater collapse; although, in the past, such models have been rarely and poorly constrained by field data from terrestrial craters. However, this is a circular argument as very few terrestrial impact structures have been studied in sufficient detail. In particular, detailed geological maps, the most important and fundamental tool of the structural geologist, are available for only a handful of craters. Most of the available maps resulted from detailed mapping campaigns of small to mid-size complex impact structures undertaken during the Apollo era (e.g., the ~6 km diameter Decaturville [Offield and Pohn 1979], ~13 km diameter Sierra Madera [Wilshire et al. 1972], and the ~12 km diameter Wells Creek [Wilson and Stearns 1968] impact structures). Recent mapping campaigns include those at the ~5 km diameter Upheaval Dome (Kriens et al. 1999) and the ~24 km diameter Gosses Bluff (Milton et al. 1996a, 1996b) impact structures. Mapping campaigns are also ongoing at the ~250 km diameter Vredefort (e.g., Lana et al. 2003; Wieland et al. 2003), and ~260 km diameter Sudbury (e.g., Spray et al. 2004, and references therein) impact structures. It should be noted that the majority of these previous investigations focused on mapping central uplifts, with relatively little work occurring in the collapsed crater rim regions.

The ~39 Ma Haughton impact structure, 23 km in diameter, is well-preserved and well-exposed due to the prevailing polar desert environment on Devon Island in the Canadian Arctic. Early structural investigations of Haughton were carried out by Bischoff and Oskierski (1988) under the auspices of the Haughton Impact Structure Studies (HISS) project (see Grieve 1988 for a summary). Mapping at Haughton over the course of six field seasons has resulted in the production of a detailed 1:25,000 scale geological map, which is included as part of this special issue. This represents the most detailed, complete geological map of a crater this size and allows an investigation of the amount and nature of deformation outward from the crater center, in the near-surface region. Key stratigraphic horizons in the ~1880 m thick series of almost flat-lying sedimentary rocks provide evidence for the depth of excavation and amount of structural uplift and deformation. This work places constraints on the tectonic evolution and formation of Haughton and of the kinematics and mechanics of complex impact crater formation in general.

GEOLOGICAL SETTING OF THE HAUGHTON IMPACT STRUCTURE

Haughton is a well-preserved complex impact structure 23 km in diameter that is situated on Devon Island in the Canadian Arctic Archipelago (75°22'N, 89°41'W) (Fig. 1). Recent ⁴⁰Ar-³⁹Ar dating of potassic glasses yields an age of 39 ± 2 Ma (Sherlock et al. 2005) for the Haughton impact event. The pre-impact target sequence at Haughton comprised a ~1880 m thick series of Lower Paleozoic sedimentary rocks of the Arctic Platform, overlying Precambrian metamorphic basement rocks of the Canadian Shield (Figs. 1 and 2) (Frisch and Thorsteinsson 1978; Thorsteinsson and Mayr 1987a; Osinski et al. 2005a). The unmetamorphosed sedimentary succession consists of thick units of dolomite and limestone, with subordinate evaporite horizons and minor shales and sandstones (Fig 1b) (Thorsteinsson and Mayr 1987a, 1987b). This stratigraphically conformable sequence of early Cambrian to Siluro-Devonian rocks lies in a gently west-dipping homoclinal succession, which exposes approximately north-south striking layers that young to the west (Fig. 1a).

Allochthonous crater-fill deposits form a virtually continuous 54 km² unit covering the central area of the structure (Fig. 2) (Redeker and Stöffler 1988; Osinski et al. 2005b). Recent field and analytical scanning electron microscopy (SEM) studies indicate that these rocks are carbonate-rich impact melt breccias (Osinski and Spray 2001, 2003; Osinski et al. 2005b). The impact melt breccias have a maximum current thickness of ~125 m, although the presence of this unit up to ~140 m above the central topographic low area suggests that the original thickness was >200 m (Osinski et al. 2005b). Isolated outcrops up to a radial distance of ~6 km from the crater center further suggest that the crater-fill originally completely occupied the central area of the crater (Osinski et al. 2005b). The crater-fill impact melt breccias and, in places, the Paleozoic target rocks, are unconformably overlain by the Haughton Formation, a series of post-impact lacustrine sediments (Fig. 2; map insert). These sediments consist of dolomitic silts and muds with subordinate fine-grained dolomitic sands (Hickey et al. 1988). Recent studies suggest that the Haughton Formation was laid down 10⁵–10⁶ yr following the impact event, after a substantial amount of erosion of impact melt breccias and pre-impact target rocks (Osinski and Lee 2005).

Haughton is associated with a negative Bouger gravity anomaly ~24 km in diameter (Pohl et al. 1988). The center of the Haughton structure is associated with a minimum of ~3 mgal with very steep gradients surrounded by weaker relative maxima at ~6–7 km radial distance (Pohl et al. 1988). The overall negative anomaly has been explained as a bowl-shaped zone with reduced densities as compared to the undisturbed surroundings (Pohl et al. 1988). A ground survey revealed a 300 nT positive magnetic anomaly at the geometric center of Haughton (Pohl et al. 1988), which has been

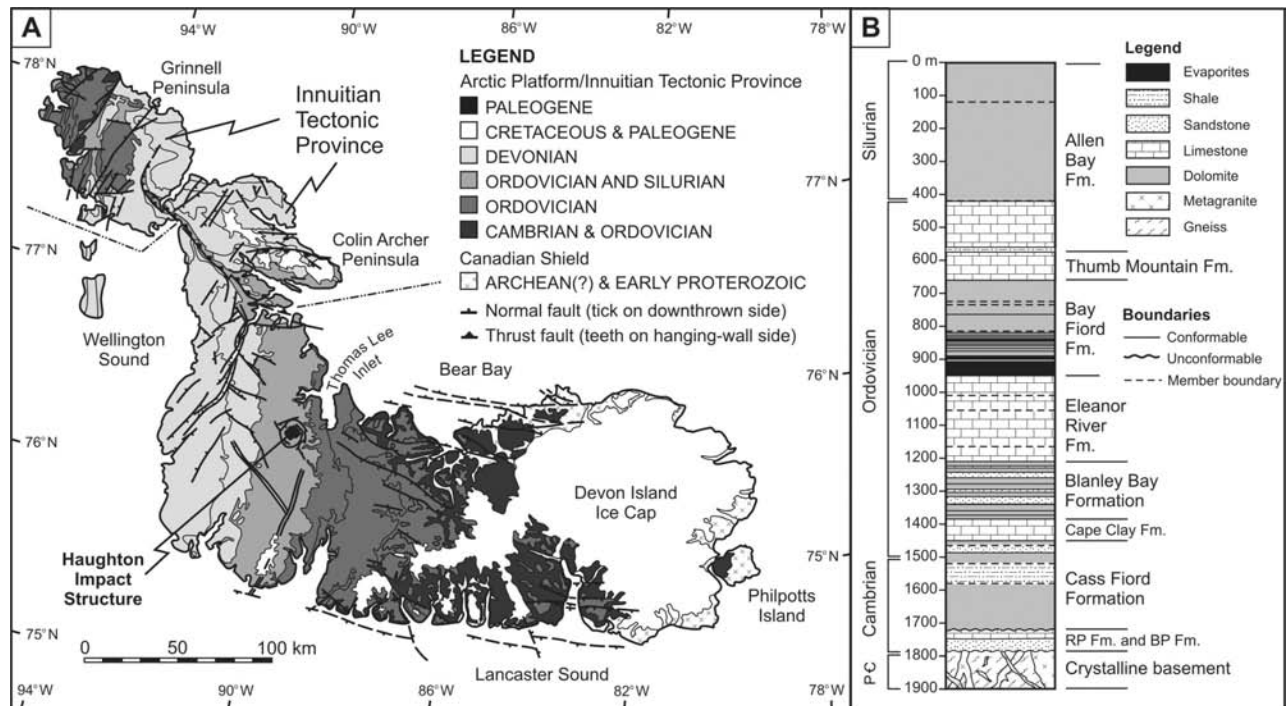


Fig 1. a) A geological map of Devon Island, after Okulitch (1991). b) A stratigraphic column showing the pre-impact target sequence at the Haughton impact structure. Compiled with field data from Thorsteinsson and Mayr (1987a) and G.R.O. Abbreviations: Fm. = Formation; RP = Rabbit Point; BP = Bear Point.

confirmed by recent airborne magnetic surveys (Glass et al. 2005). The positive magnetic anomaly coincides with the central negative gravity anomaly and may be equated with the presence of a core of very low-density material (Pohl et al. 1988).

PRE-IMPACT STRUCTURAL SETTING OF HAUGHTON

Devon Island is situated in the eastern part of the Canadian Arctic Archipelago and is underlain by rocks from three geological provinces (Fig. 1a): (1) the Canadian Shield; (2) the Arctic Platform; and (3) the Innuitian Tectonic Province. Haughton lies south of the southernmost structural boundary of the Innuitian Tectonic Province (Fig. 1a). Therefore, the tectonics of this province can essentially be disregarded for the purpose of this study. The Arctic Platform and the Canadian Shield have been characterized by relative stability since the end of Precambrian time and together they constitute part of the North American craton (Dawes and Christie 1991).

The Arctic Platform and Canadian Shield of Devon Island are cut by numerous and commonly extensive normal faults (Thorsteinsson and Mayr 1987a, 1987b). These faults, excluding those associated with the Haughton structure, have been divided into two main areally separated systems (Fig. 1a). In the west of Devon Island the regional trend is approximately northeast-southwest, whereas further to the

east the trend is essentially northwest-southeast (Frisch and Thorsteinsson 1978; Thorsteinsson and Mayr 1987a, 1987b). Some faults of both systems form grabens that preserve sedimentary rocks of the Cretaceous Eureka Sound Formation, which suggests that these sediments may have been more widely distributed than their present outcrop suggests (Frisch and Thorsteinsson 1978).

SUBSURFACE STRUCTURE OF HAUGHTON

The subsurface structure of Haughton has been imaged with a single seismic reflection profile that runs from the “undisturbed” Allen Bay Formation carbonates in the northwest to within ~2.3 km of the geometric center of the structure (Fig. 3) (Hajnal et al. 1988; Scott and Hajnal 1988). Ten reflecting horizons were correlated with the Paleozoic sedimentary sequence of Devon Island via a sonic log (Scott and Hajnal 1988). Due to the absence of local borehole information, the correlation of markers was achieved by combining information on the regional geology and several distant sonar logs (Hajnal et al. 1988).

Hajnal et al. (1988) estimated the total thickness of sedimentary strata to be ~1885 m, which is in agreement with field studies (~1880 m) (Frisch and Thorsteinsson 1978; Osinski et al. 2005a). However, it should be noted that there are discrepancies between the thickness of certain formations based on field mapping and from seismic studies. In particular, field studies show that the Allen Bay Formation is

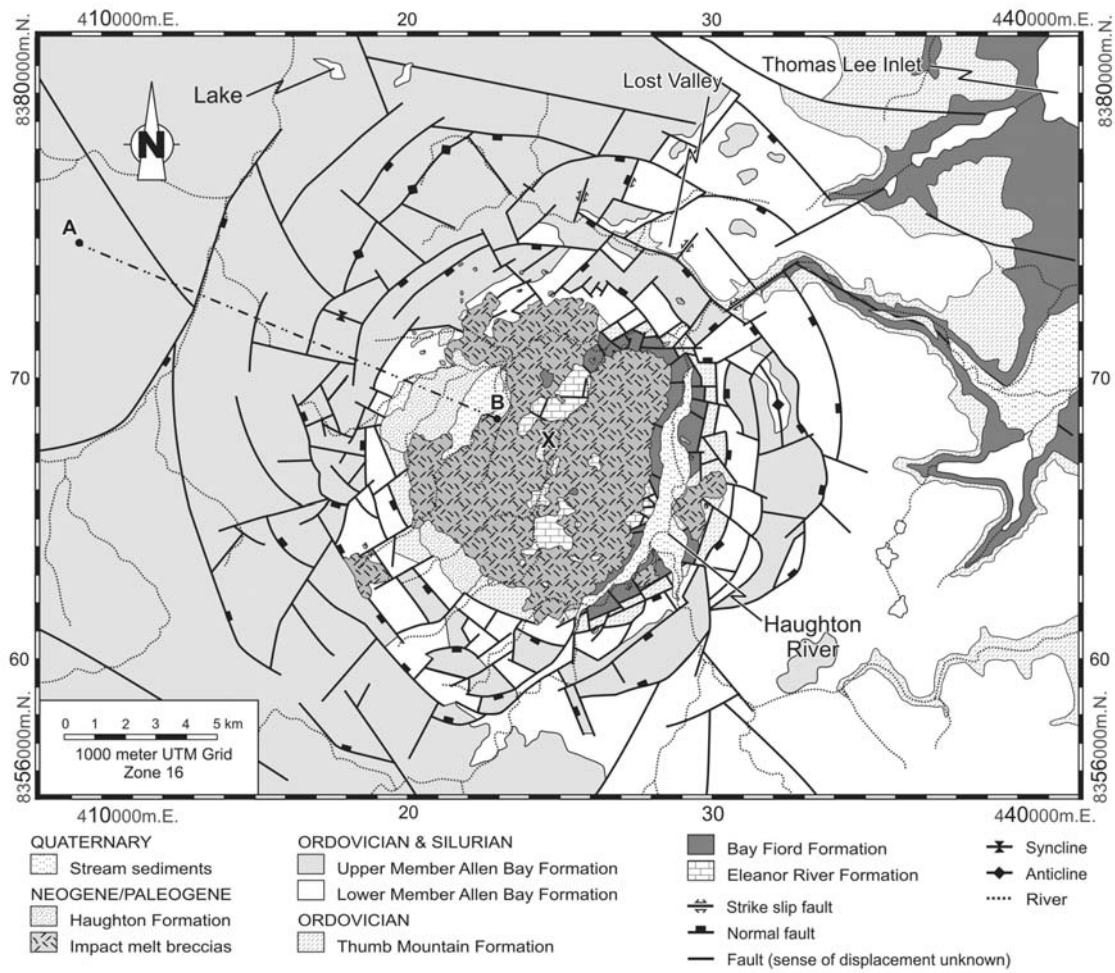


Fig. 2. A simplified geological map of the Haughton impact structure. See map insert for detailed version. Lithological data >15 km radial distance from the center of the structure are from Thorsteinsson and Mayr (1987b). "X" = Anomaly Hill. Line A-B is the approximate trace of the seismic line shown in Fig. 3.

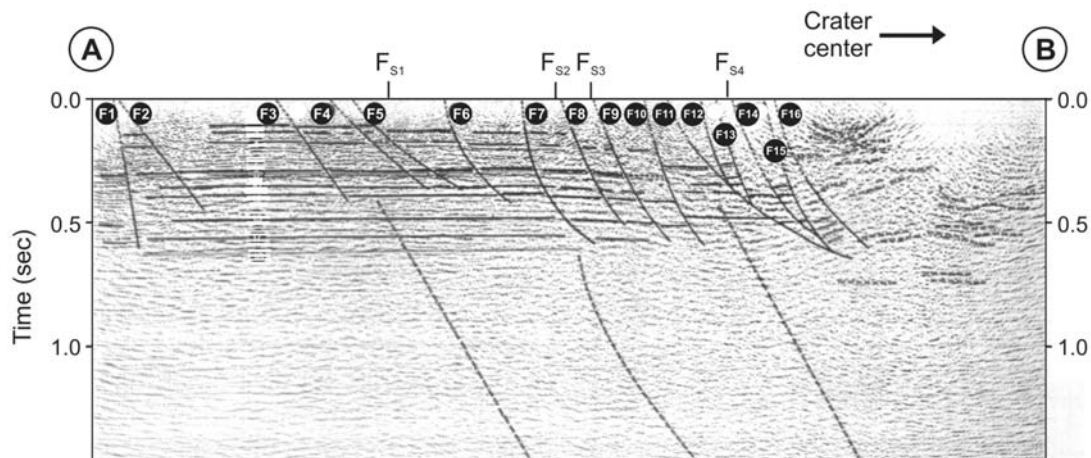


Fig. 3. Interpreted seismic section for the Haughton impact structure modified from Scott and Hajnal (1988). See Fig. 2 for location. Locations of surface mapped faults (FS1 to FS4) are those of Robertson and Sweeney (1983). F1 to F16 are faults identified from the reflection data. Stratigraphic correlations east of fault F9 are tentative only. Short dashed lines indicate uncorrelatable seismic energy. Sub-vertical dashed lines mark changes observed in the general character of the deeper portion of the section. Due to the low signal-to-noise conditions, the origin of these patterns was not established. The east end of the profile is ~2.3 km from the geometric center of Haughton.

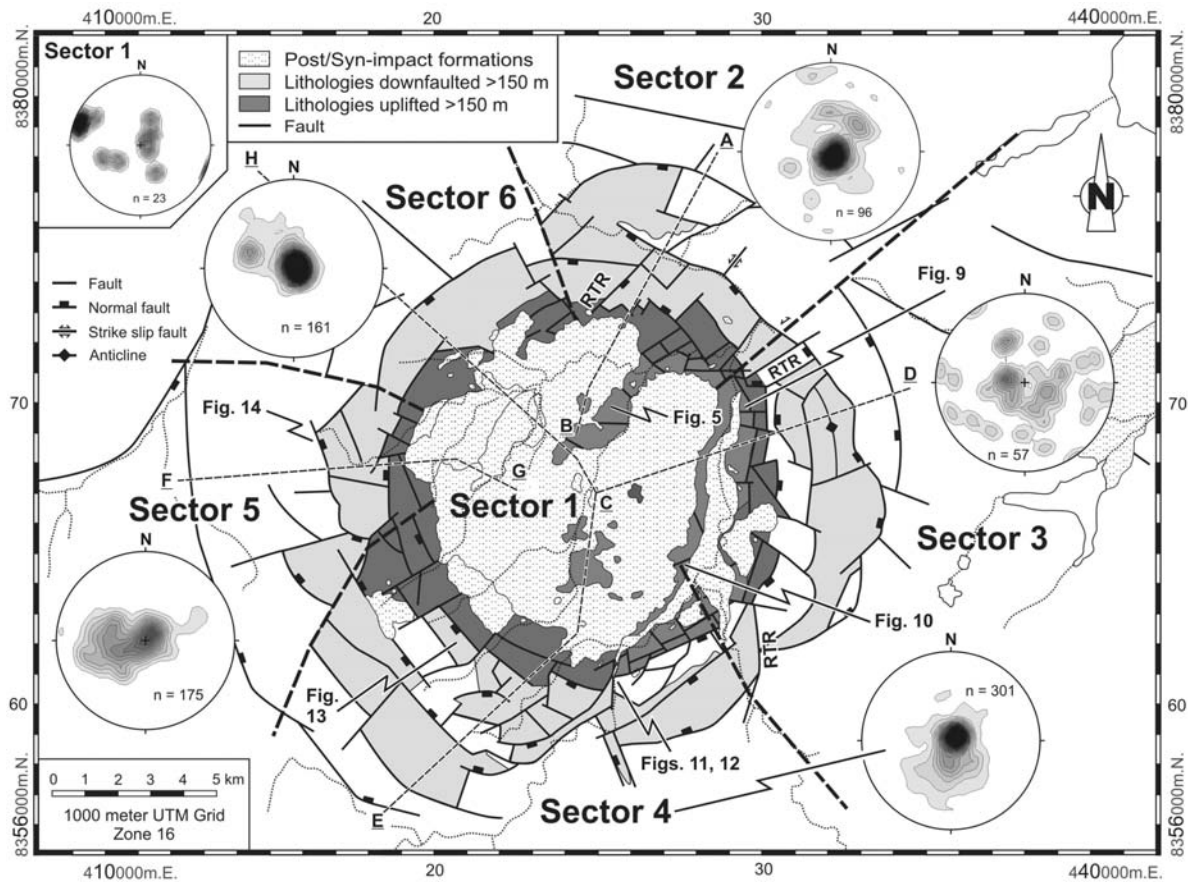


Fig. 4. A simplified structural map of the Haughton impact structure showing the six main structural sectors defined in this study. Structural data for each sector are plotted on equal-angle stereonet as poles to bedding (n = number of data points). In this method, vertical beds will plot on the circumference, while horizontal strata will plot at the center of the stereonet. RTR = radial transpression ridge. The lines of the cross sections in Fig. 6 are plotted as dashed lines.

~650 m thick, and that the thickness of strata between the base of the Eleanor River Formation and the Precambrian surface is ~570 m (Thorsteinsson and Mayr 1987a). In contrast, Hajnal et al. (1988) estimated the same values to be ~910 m and ~140 m, respectively. Thus, the interpretation of markers in Fig. 3 may be incorrect. The important findings of the seismic studies are summarized below (Hajnal et al. 1988; Scott and Hajnal 1988):

1. The quality of coherent reflection signals deteriorates rapidly toward the center of the structure.
2. Seismic studies reveal the presence of a complex fault system within the western half of the Haughton structure, a feature not revealed by previous surface structural studies (Bischoff and Oskierski 1988).
3. Concentric normal faults at ~12 km radius suggest that Haughton has an apparent diameter of ~24 km, assuming that the distribution of faults is the same around the entire structure.
4. The characteristics of the faulting change toward the center of the structure. In particular, there is a general increase in the spatial density, penetration depth and the amount of vertical movement on these faults.
5. Significant continuation of any fractured zones into the crystalline basement beneath the crater was not detected in the seismic study.
6. The first indication of a possible upturning of fragmented blocks occurs ~5.5 km from the center of the structure.
7. The sedimentary target rocks, with seismic velocities of ~5800–6300 ms^{-1} , represent very competent lithologies with strength characteristics comparable to the underlying crystalline basement (~5700–6100 ms^{-1}).

STRUCTURAL SECTORS OF THE HAUGHTON IMPACT STRUCTURE

Haughton consists of a dome-like arrangement of sedimentary strata, with the oldest rocks exposed in the center, surrounded by concentric fault-bounded blocks of progressively younger Paleozoic formations (Figs. 2 and 4; map insert) (Frisch and Thorsteinsson 1978; Robertson and Sweeney 1983; Bischoff and Oskierski 1988). Detailed 1:10,000 to 1:25,000 scale mapping has resulted in the generation of a new geological map of Haughton that shows the structure in greater detail (see map insert). Six



Fig. 5. A panoramic field image showing a series of fault-bounded blocks of the Bay Fiord Formation, overlying Eleanor River Formation strata of the central uplift. Solid and dashed lines represent faults and bedding surfaces, respectively. Kinematic indicators record the following sequence of structural events: (1) displacement of several large “plates” of Bay Fiord Formation strata in toward the crater center (i.e., toward the left of the image); (2) shortening and duplication of beds along thrust faults and folds in the hanging-walls (e.g., right of image) of these faults; (3) minor extensional outward-directed movement. UTM 425,300 m.E. 8,370,000 m.N.

distinct structural sectors are recognized at Haughton (Fig. 4). These will be described in detail below. Note that the six sectors defined here are based on detailed mapping and represent different structural domains, unlike the “sectors” of Bischoff and Oskierski (1988), which represent areas they selected for field studies.

Sector 1: Central Area

The central area of the Haughton structure (<4 km radial distance from the crater center) comprises a shallow basin, ~200 m lower in elevation than the surrounding plateau, and a series of topographic highs (the “interior peaks” of Robertson and Sweeney 1983), which consist of irregularly bedded grey limestones with interbedded black chert nodules of the Eleanor River Formation (Figs. 2 and 4). These lithologies have been uplifted >1050 to <1300 m above their pre-impact stratigraphic position and they generally display dips of ~10–40° (Fig. 4; map insert). However, it is often not possible to measure the orientation of these lithologies due to the irregular, wavy nature of the original bedding surfaces. Shatter cones were found in all exposures of the Eleanor River Formation in sector 1. In addition, these lithologies are typically extensively brecciated; however, it is notable that there is typically no observable offset or rotation of clasts (i.e., the original sedimentary structures are preserved). In this respect, these intensely fractured rocks resemble the “Gries structure” seen at the Ries impact structure, Germany (e.g., Chao et al. 1978). These brecciated masses at Haughton have also been cemented, commonly by post-impact hydrothermal solutions (Osinski et al. 2005c).

Mapping reveals the presence of several fault-bounded blocks of gently dipping (up to ~30°) Bay Fiord Formation strata overlying the Eleanor River Formation in this central region (Fig. 2; map insert). Kinematic indicators (e.g., microfaults, asymmetric folds within anhydrite and gypsum) record evidence for inward compressional movement (i.e., thrusting), and subsequent, minor outward-directed extensional movement (e.g., Fig. 5). Deformation has reduced

the Bay Fiord Formation evaporites to a megabreccia in places.

Impact melt breccias occur within a radius of ~1 km from the geographic center of the Haughton structure, though exposure of bedrock is generally poor (Fig. 2). However, two large coherent blocks of steeply dipping sandstone are present and these can be assigned to the Blanley Bay Formation. These blocks have been uplifted >1300 to <1450 m above their pre-impact stratigraphic positions (map insert). Bischoff and Oskierski (1988) also noted the presence of poorly bedded limestones that could belong to the Cass Fiord Formation, although this stratigraphic assignment is very tentative.

Sector 2: Northern Sector

The northern sector contains some of the best exposed structural features at Haughton. It is subdivided into two distinct zones. The innermost region is marked by intensely faulted and fractured lithologies of the Bay Fiord and Thumb Mountain formations (Figs. 2, 4, and 6a; map insert). The present-day outcrops have been uplifted by >300–<700 m and >200–<400 m, respectively, above their pre-impact stratigraphic position (Fig. 2). There is a noticeable change in strike of these lithologies toward the crater center from ~ESE-WNW or E-W (i.e., a concentric orientation) to ~NE-SW or NNE-SSW (i.e., a radial orientation) (map insert). In addition, many of these beds are overturned. (Note that many more outcrops may be overturned; however, the absence of fossil horizons and other markers does not allow unequivocal verification.) Exposure of fault surfaces is very limited in these areas; however, differences in bedding orientations and lithology across many fault traces, allows some insight. In particular, the majority of the radial “faults” mapped in the innermost region appear to be either steeply dipping oblique reverse faults, or may be best described as the axial traces of tight, chevron-style folds (i.e., folding whereby planar fold limbs meet at a discrete, sharp hinge).

The intensely faulted inner region of this sector changes

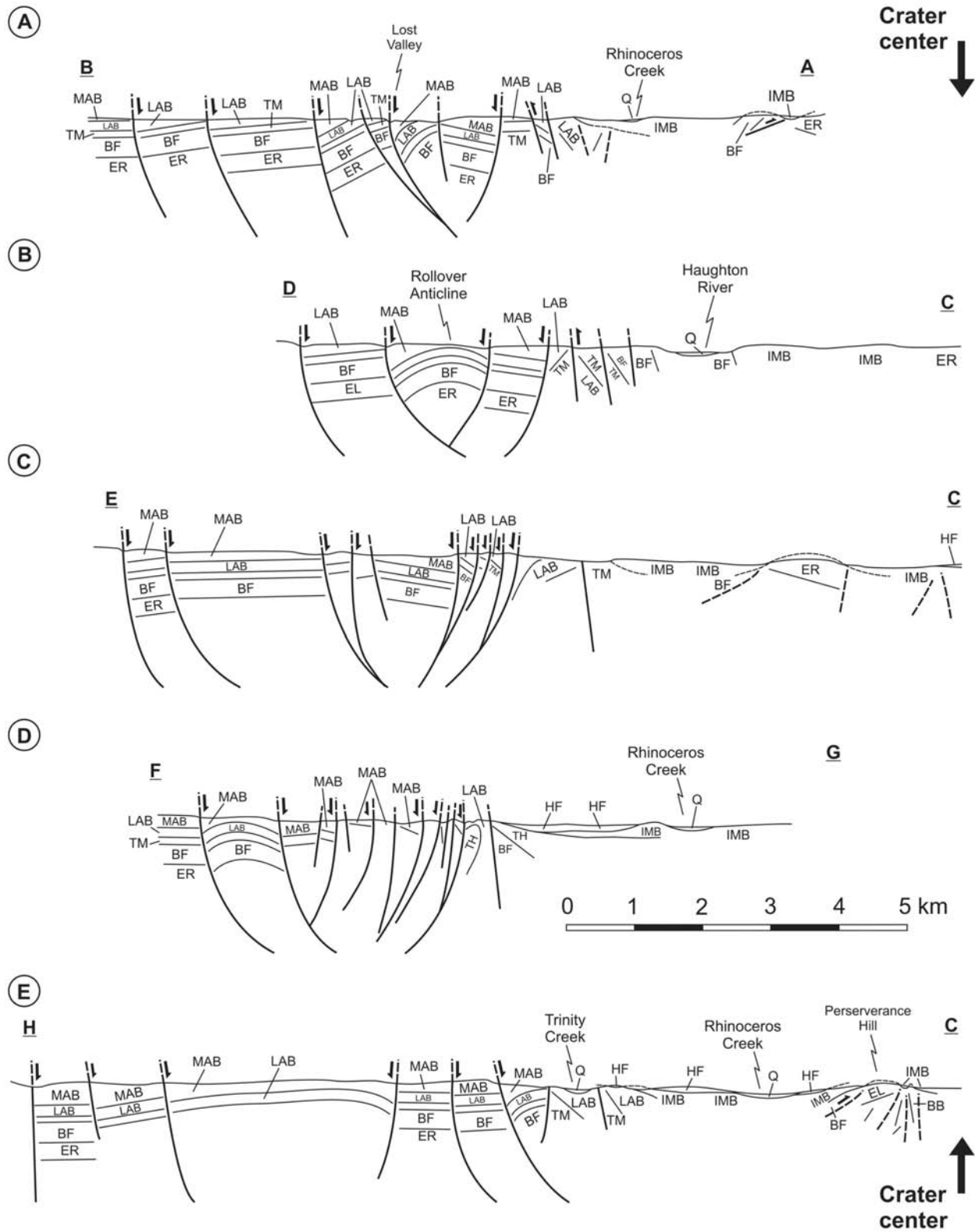


Fig. 6. A series of cross-sections across the Haughton structure. The right-hand edge of the page corresponds to the center of the structure. See Fig. 4 for location of sections. Q = Quaternary deposits; HF = Haughton Formation; IMB = impact melt breccias; MAB = Middle Member Allen Bay Formation; LAB = Lower Member Allen Bay Formation; TM = Thumb Mountain Formation; BF = Bay Fiord Formation; ER = Eleanor River Formation; BB = Blanley Bay Formation.

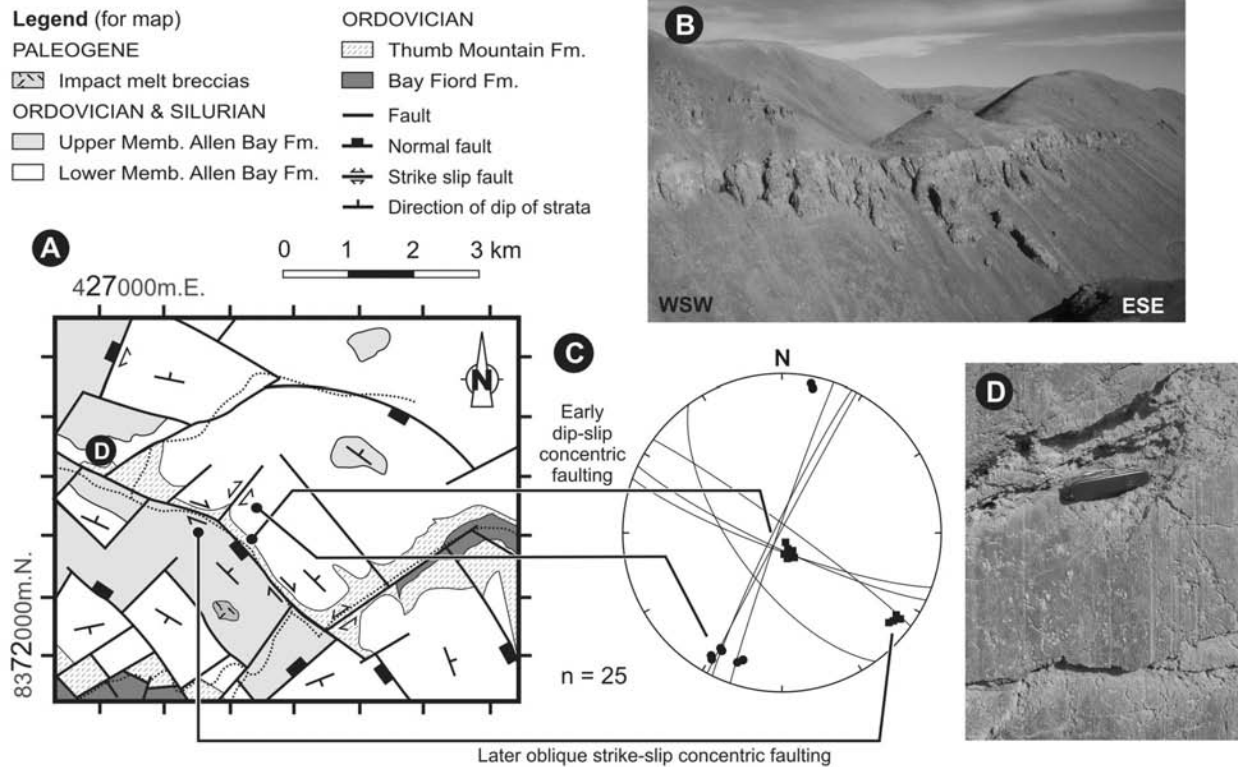


Fig. 7. a) A geological map of the Lost Valley region in the northeast of the Houghton structure. b) An aerial view looking to the northeast of a series of concentric fault surfaces exposed in the northern wall of the Lost Valley. c) Slickenside lineations from fault surfaces are plotted on an equal-angle stereonet. In this method, vertical lineations will plot at the center of the stereonet, while horizontal lineations will plot at the circumference. Circles represent data from radial faults and squares from concentric faults. Note that radial faults record evidence for low-angle oblique strike-slip movement. Concentric faults record evidence for two phases of deformation. d) A close-up field photograph showing well-developed slickenside lineations that record normal dip-slip movement.

passing outward into a series of larger fault-bounded blocks comprising different levels of the Allen Bay Formation (Figs. 2, 4, and 6a). Strata dip both inward and outward from the crater center (map insert). Deformation in this sector is concentrated into the major faults zones, with very little fracturing, faulting, or brecciation within the interior of the fault-bounded blocks. Two large blocks of the Lower Member of the Allen Bay Formation have been down-dropped and rotated so that bedding dips in toward the crater center (bottom left corner of Fig. 7a; map insert). This requires movement on listric extensional fault surfaces that dip outward from the crater center.

The dominant structural feature in sector 2 is a large inward-dipping listric extensional fault that forms the “Lost Valley” (Figs. 4, 6a, 7, and 8). Here, the Middle Member of the Allen Bay Formation is juxtaposed with the Thumb Mountain Formation indicating vertical displacement of >250–<450 m (Figs. 2, 6a, 7a, and 7b). This feature, therefore, represents a “superfault,” using the terminology of Spray (1997). Rotation of bedding in the hanging-wall can be up to ~50–70° from the original sub-horizontal orientation (map insert). Exposure is excellent in this region and allows a detailed look at the relationship between the concentric and

radial fault systems (Fig. 7). Slickenside lineations and careful lithological mapping reveals that two episodes of movement occurred along the concentric fault surfaces: (1) early, major, top down-to-the SSW high angle extension (Figs. 7a–d); and (2) later top down-to-the SE oblique strike-slip extensional movement (Figs. 7a and 7c). This later movement resulted in up to ~400 m horizontal dextral offset of several major radial faults (e.g., the offset of a fault marked by the Houghton River, along the Lost Valley) (Figs. 2, 4, and 7a; map insert). There is, therefore, a clear temporal relationship between radial and concentric faulting in this sector. Outward from this major listric fault, there is a decrease in the spatial intensity of faulting. In general, large kilometer-size blocks dip gently outward, indicating displacement along inward-dipping listric extensional faults.

Radial faults in this outer zone display oblique strike-slip slickenside lineations (Figs. 4 and 8c; map insert). Large thicknesses of fault breccia (up to ~8 m) are commonly present along these radial faults indicating substantial movement; however, marker horizons indicate that very little (typically <5 m) overall displacement has occurred (i.e., substantial repeated back-and-forth movement occurred along these faults).



Fig. 8. An airborne X-band radar image of the Haughton impact structure. The field of view is ~40 km across. Image courtesy of the Geological Survey of Canada.

Sector 3: Eastern Sector

The eastern sector of the Haughton structure is characterized by a series of large, kilometer-size fault-bounded blocks of the Middle Member of the Allen Bay Formation that have been down-dropped >50–250 m so that they are now juxtaposed with the Lower Member of the same formation (Figs. 2, 4, and 6b; map insert). Exposure is poor in this region; however, lithological differences between the Lower (predominantly limestone) and Middle members (predominantly dolomite), and changes in the bedding orientation, allow structural information to be gleaned.

The major tectonic feature in this sector is a continuation of the “Lost Valley fault” from sector 2 (Fig. 4). The rotation of strata in the hanging-wall by up to ~80° indicates that this feature is also an inward-dipping listric extensional fault. A large rollover anticline is present in the hanging-wall of this fault (Figs. 2 and 6b; map insert). As with sector 2, the outermost concentric faults are all inward dipping; whereas the innermost concentric faults typically dip outward from the crater center. Thus, the strata tend to dip away from the crater center in the outermost regions and inward as the crater center is approached (cf. Bischoff and Oskierski 1988). As with sector 2, the majority of deformation in this outer zone is concentrated into the major faults, with very little fracturing, faulting, or brecciation within the individual fault-bounded blocks. However, several sub-vertical dykes of monomict breccia have been recognized in this sector, in contrast to sector 2 where these features are rare (cf. Bischoff and Oskierski 1988). It is not clear at present whether the dyke-forming material is autochthonous (i.e., fault-related cataclaste or pseudotachylyte), or allochthonous (i.e., injected impact melt or impact breccias).

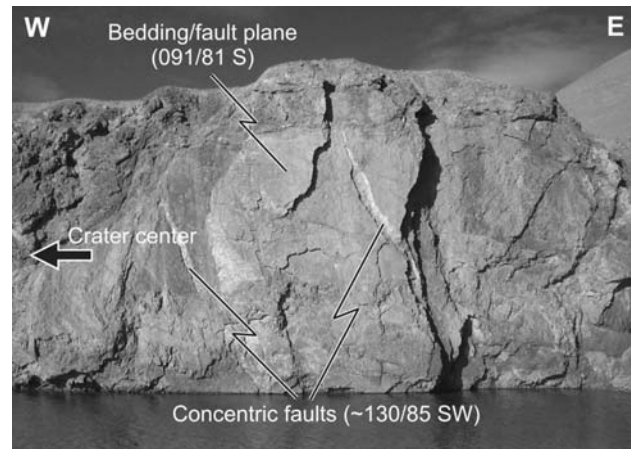


Fig. 9. A field photograph of sub-vertical, uplifted, and overturned strata of the Thumb Mountain Formation along the Haughton River (see Fig. 4 for location). The following sequence of structural events can be established: (1) uplift and rotation of beds; (2) activation of bedding surfaces as faults; (3) oblique strike-slip movement (trend ~090°) along bedding-parallel fault planes; and (4) movement along sub-vertical concentric faults that cut bedding surfaces at oblique angles (~130° trend). UTM 429,280 m.E. 8,370,590 m.N.

A positive flower structure, a form of radial transpression ridge (Kenkmann and von Dalwigk 2000), occurs at the extreme northern end of this sector, to the south of the Haughton River (Fig. 4). This is manifest as a structural high within the Lower Member of the Allen Bay Formation (Fig. 4; map insert). A further possible positive flower structure occurs in the southern part of this sector.

Moving inward toward the crater center, highly fractured and faulted lithologies of the Bay Fiord and Thumb Mountain formations display steep to overturned orientations in a zone ~5.5–6.0 km in radius with respect to the crater center (e.g., Figs. 4, 6b, and 9). Breccia dykes (monomict and polymict) are common in this zone (cf. Bischoff and Oskierski 1988). There are some excellent exposures along the Haughton River that allow detailed outcrop scale investigation of structural features (e.g., Fig. 9).

Along most of its length, the west side of the Haughton River is characterized by a series of outcrops of uplifted Bay Fiord Formation evaporites that are draped by impact melt breccias. These lithologies are typically folded, as noted by Bischoff and Oskierski (1988). However, fieldwork carried out by G.R.O. in the undisturbed target sequence outside the crater reveals that some lithologies beyond the crater are also folded, so that it is not possible to discriminate between pre-impact and impact-related folds in these outcrops. At many locations, pervasive microfaults clearly cross-cut fold fabrics. The majority of these features (>90%) record evidence for thrusting in toward the crater center.

Near the junction of the west and east forks of the Haughton River, a very complex structural array of different lithologies is revealed (Fig. 10; map insert). Strata of the Eleanor River Formation, restricted to the central zone in all

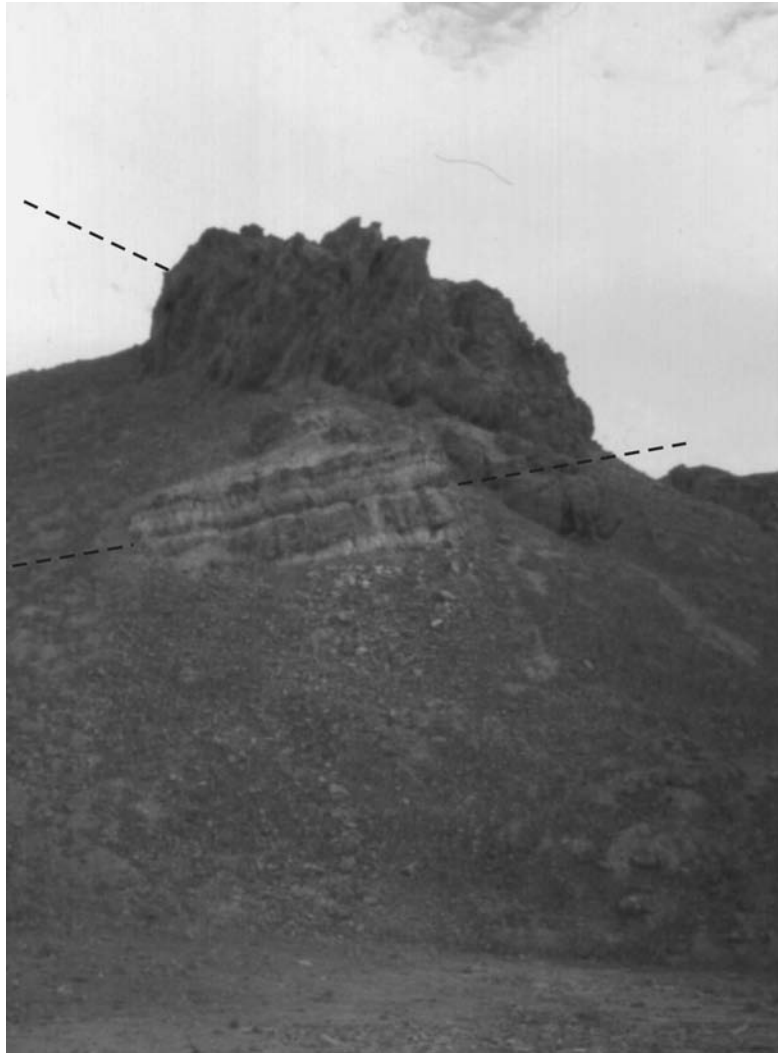


Fig. 10. Field photograph looking to the northeast of a ~60 m high cliff section along the Houghton River valley (see Fig. 4 for location). Well-bedded, cream-colored limestones from the upper part of the Bay Fiord Formation (foreground) are juxtaposed with massive limestones of the Eleanor River Formation (rear). These lithologies occur at the outer edge of the central uplift and have been uplifted by >750 to <1000 m and >500 to <600 m, respectively. Dashed lines indicate bedding. UTM 423,600 m.E. 8,359,900 m.N.

other regions, extend out to ~4.5 km from the crater center (Figs. 2 and 4; map insert). In addition, fault-bounded blocks of different levels of the Bay Fiord Formation are juxtaposed with the Eleanor River Formation (Fig. 10).

Sector 4: Southern Sector

The southern structural sector of Houghton is characterized by a distinctly different style of deformation compared to sectors 2 and 3. In particular, the majority of concentric faults dip outward from the crater center (Figs. 2, 4, 6c, 11, and 12; map insert). This accounts for the curious inward dip of the sedimentary formations in this area, as noted by previous workers (Bischoff and Oskierski 1988). It is only the outermost major concentric faults that dip inward (cf. sectors 2 and 3 where the majority of fault surfaces dip in

toward the crater center). Several crestal collapse grabens are present where inward- and outward-dipping listric faults meet (an example of which in this sector preserves impact melt breccias: Figs. 2, 4, and 6c).

Concentric fault planes display evidence for two episodes of movement (cf. sector 2). The first is a major episode of top down-to-the SE to S high angle extension (i.e., away from the crater center) (Fig. 11). The offset of marker beds by up to ~200 m and the presence of >50 m thickness of fault breccias (e.g., Fig 12) indicate that this early phase of deformation was major. Later, minor movement involved top-down to the NNE and SSW oblique strike-slip movement (Fig. 11). There is typically little deformation of the country rocks outside the main faults, aside from the minor development of microfaults and cataclastic veins (up to ~2–4 cm across).

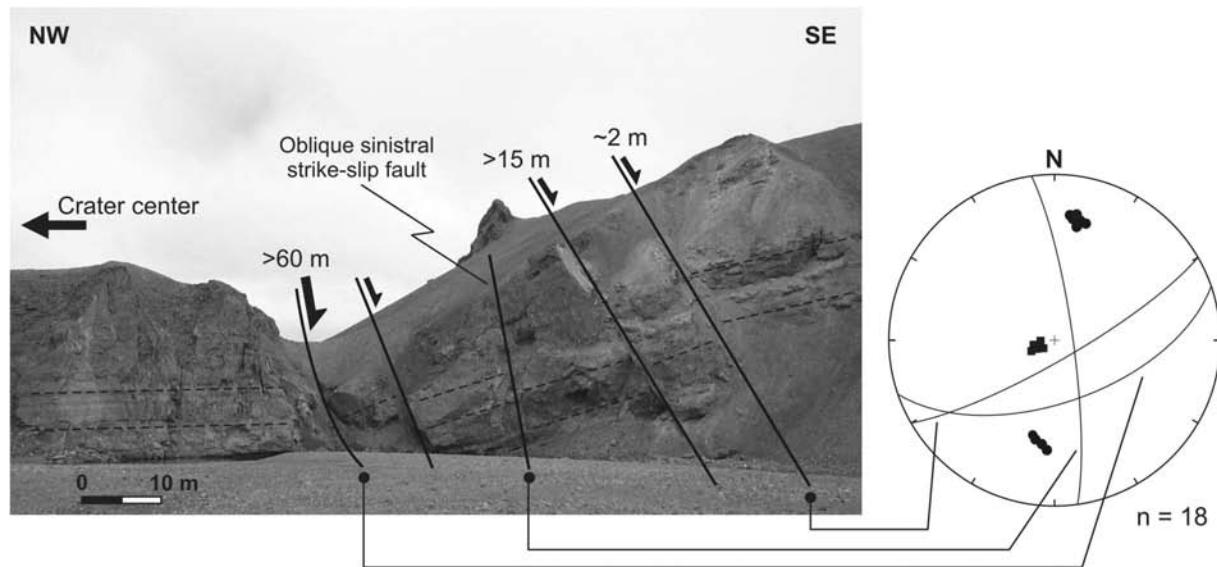


Fig. 11. Field photograph showing a series of concentric faults dipping outward from the crater center (see Fig. 4 for location). The solid and dashed lines represent faults and bedding surfaces, respectively. Slickenside lineations from fault surfaces are plotted on an equal-angle stereonet. In this method, vertical lineations will plot at the center of the stereonet, while horizontal lineations will plot at the circumference. Two episodes of fault movement are indicated: (1) top down-to-the SE to S high angle extension (squares); and (2) later, minor top down-to-the NNE and SSW oblique strike-slip movement (circles). UTM 427,600 m.E. 8,365,100 m.N.

At a radius of ~ 5.5 – 6.5 km, with respect to the crater center, there is a zone of highly faulted and fractured and, in places, overturned beds (Figs. 6c and 13). Bedding-parallel detachment faults have been observed in sector 4 at radial distances from the crater center of ~ 5.0 – 9.5 km (e.g., Fig. 13). Stepped surfaces and slickenside lineations record evidence for outward-directed movement of the hanging-wall blocks. These detachment faults are cut, offset, and rotated by later sub-vertical concentric faulting.

Radial faults are common in the outermost part of this sector and these typically display oblique strike-slip slickenside lineations. Two main types can be recognized: (1) faults with large thicknesses of fault breccia (up to ~ 6 m), but that record little overall displacement (typically < 10 m), suggesting repeated back and forth movement (cf. sector 2); and (2) oblique strike-slip faults that record significant displacement (up to several tens of meters). It is apparent that the former radial faults are always cut and offset by concentric faults, whereas the latter can cut concentric faults. As the crater center is approached, radial faults *sensu stricto* are scarce. Instead, many of the faults change strike significantly and are neither radial or concentric in orientation.

Sector 5: Southwestern Sector

The southwestern area of Haughton is a highly complex structural region. The long, arcuate concentric listric faults seen in other regions of the crater are typically absent (Figs. 2 and 4; map insert). Instead, this sector is characterized by a pervasive series of closely spaced faults with highly variable orientations with respect to the crater center (Figs. 2, 4, and

6d; map insert). Major and minor concentric fault planes dip outward from the crater center in the interior part of this zone, with extensional top down-to-the W-SW displacement (e.g., Fig. 14). This is consistent with the inward tilting of strata in the hanging-walls of these faults. The outermost concentric faults in this sector are listric extensional faults dipping in toward the crater center. A large rollover anticline is present in the hanging-wall of the outermost listric fault (map insert). Compared with other sectors, there is an increase in brecciation and development of cataclastic veins and microfaults in this sector.

The nature of radial faulting is distinctly different in this sector. Approximately half of the mapped radial faults are listric extensional faults, in contrast to other sectors where oblique strike-slip radial faulting predominates. The remaining radial faults appear to be either steeply dipping oblique reverse faults, or to represent the axial traces of tight, chevron-style folds. As with the other sectors, at a radius of ~ 5.0 – 6.0 km from the crater center, there is a zone of steeply dipping and commonly overturned strata that are uplifted above their pre-impact stratigraphic setting.

Sector 6: Northwestern Sector

A series of isolated exposures bordering the impact melt breccias in sector 6 indicates that the strongly disturbed structural zone at ~ 5.0 – 6.5 km radial distance from the crater center is continuous around the Haughton structure (map insert). In this zone, strata of the Lower Member of the Allen Bay Formation are uplifted up to ~ 300 m above their pre-impact stratigraphic position (Fig. 2; map insert). Two small

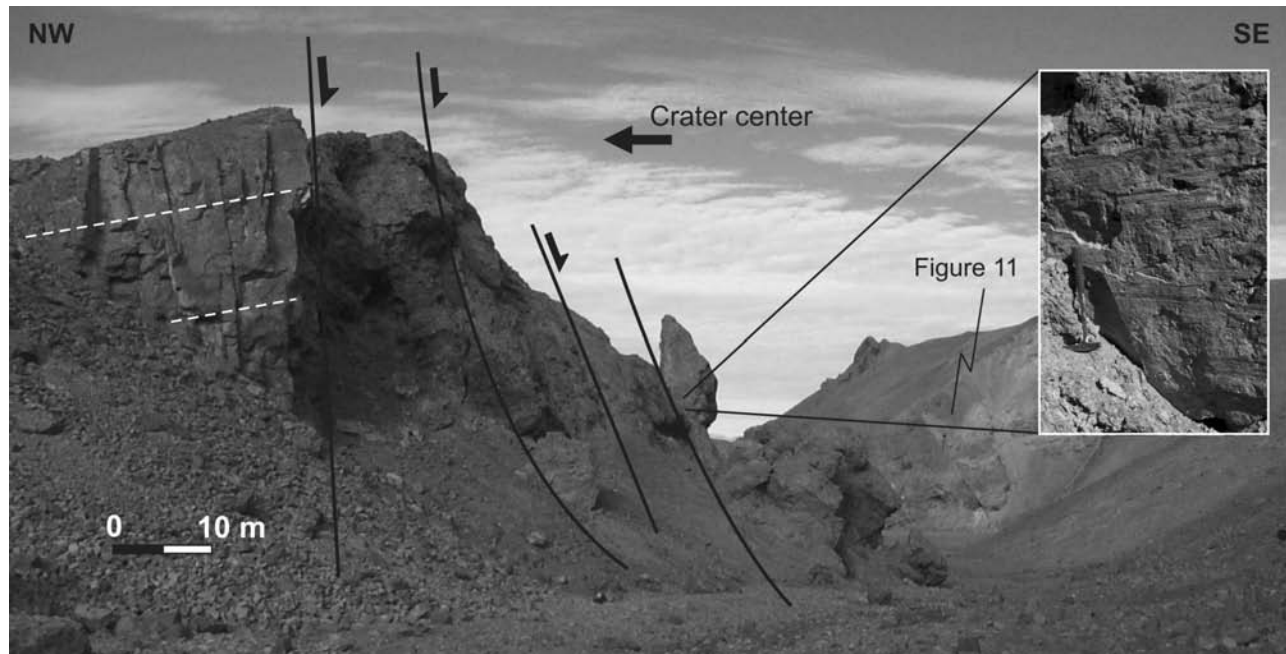


Fig. 12. A field photograph looking along the strike of concentric faults from Fig. 11. Over 40 m in thickness of fault breccia is found at this locality and is related to top down-to-the SE to S high-angle extension. The solid and dashed lines represent faults and bedding surfaces, respectively. Later, minor fault surfaces record oblique strike-slip movement (see slickenside lineations in inset). UTM 423,100 m.E. 8,359,700 m.N.

outliers of Thumb Mountain Formation are also present (map insert). These are highly fractured and overturned, and it is not clear whether they represent fault-bounded blocks or if they are ejected megablocks. To account for the relationship with surrounding country rocks in the first scenario, the Thumb Mountain Formation strata must represent thrust-faulted blocks emplaced along outward-directed vectors.

The Middle Member of the Allen Bay Formation forms the bulk of the faulted crater rim in the northwestern sector (Fig. 2). This unit typically displays gentle dips throughout most of this region (Figs. 4 and 6e; map insert). Displacement along the majority of concentric faults is typically <50 m, and often substantially less. Low amplitude folding is common, with fold axes displaying both concentric and radial orientations (Fig. 2; map insert). The fault-bounded blocks in this region, excluding the faults themselves, record little or no impact-related deformation.

DISCUSSION AND CONCLUSIONS

New mapping and detailed structural studies build on previous work at Houghton by Bischoff and Oskierski (1988). These studies provide important insights into the mechanisms and kinematics of crater rim collapse and central uplift formation in mid-size complex impact structures (e.g., ~15–30 km). These processes occur during the final (modification) stages of crater formation and remain one of the least understood aspects of the cratering process. In agreement with previous studies, Houghton can be described as

consisting of a dome-like arrangement of sedimentary strata, with the oldest rocks exposed in the center, surrounded by concentrically arranged fault-bounded blocks of progressively younger Paleozoic formations (Fig. 1; map insert) (Frisch and Thorsteinsson 1978; Robertson and Sweeney 1983; Bischoff and Oskierski 1988). However, new mapping reveals that Houghton is structurally significantly more complex than previously thought. In addition, detailed stratigraphic studies carried out outside the crater, together with regional mapping results not available to previous workers, allow a more precise correlation of strata within the Houghton structure.

The results of previous structural studies suggested that Houghton is markedly asymmetric (Frisch and Thorsteinsson 1978; Bischoff and Oskierski 1988) with intense faulting in the northern and eastern parts of structure, whereas the western and southern parts are apparently characterized by large (km-size) “plates” of Allen Bay Formation strata (Bischoff and Oskierski 1988). This study shows that Houghton is indeed asymmetric in terms of tectonic features, but not in the same way as proposed by previous authors. In particular, it is apparent that the western and southern parts of the structure are characterized by a similar, or even greater, spatial intensity of faults (Figs. 2 and 4; map insert), consistent with seismic reflection studies (Hajnal et al. 1988; Scott and Hajnal 1988). This study shows that Houghton can be divided into six major structural sectors and that the tectonics of crater modification are manifest differently in each.

The subsequent discussion will summarize and discuss the structural attributes of Haughton in the context of understanding the kinematics and mechanics of collapse and concomitant uplift during the formation of complex impact craters. When combined with data from other terrestrial impact sites, this allows a kinematic model for complex crater formation to be constructed.

Effect of Pre-Existing Structural Features on Crater Modification

Due to the active, geologically dynamic nature of our planet, no impact event occurs in a perfectly flawless, homogeneous target. The presence of pre-existing faults, folds, and joints in the target sequence can, therefore, play an important role in the formation of terrestrial impact structures. For example, it is apparent that the regional joint pattern has controlled the shape of the ~1.2 km diameter Meteor Crater, Arizona, which is “somewhat squarish in outline” (Shoemaker and Kieffer 1974). Meteor Crater is a simple crater and its squarish outline is due to controls exerted by the regional joint pattern during the excavation stage of crater formation (Shoemaker and Kieffer 1974). It is also evident that pre-existing faults have exerted significant control on modification stage processes in larger complex impact structures (e.g., the ~260 km diameter Sudbury impact structure; Spray et al. 2004).

With respect to Haughton, two main regional fault systems are present on Devon Island; however, the average spacing between the major faults is on the order of ~10 km (Fig. 1a), so that their effect on the tectonics of an impact structure 23 km in diameter is likely to have been minor. Indeed, field studies reveal that there is only one major pre-impact fault that appears to have been reactivated during crater collapse. This fault occurs in the extreme northeast of the Haughton structure passing through sectors 5 and 6 (Fig. 2; map insert). It is clear that this structure is significantly different to those faults generated during the impact event (e.g., it has a strike length of >30 km and is broadly linear). This fault also displays a northeast-southwest trend, which is typical for the regional faults of western Devon Island (Thorsteinsson and Mayr 1987a and 1987b).

Mechanics of Central Uplift Formation

It has long been recognized that lithologies in the center of complex impact structures are uplifted above their pre-impact stratigraphic position (e.g., Dence 1968; Grieve et al. 1981). However, the formation mechanism(s) of central uplifts is still not fully understood. Field observations at terrestrial impact structures reveal that the target rocks in central uplifts record a complicated kinematic history. Rocks originally displaced downwards and outward during transient cavity growth are subsequently transported inward and



Fig. 13. A field photograph from sector 4 showing the zone of sub-vertical strata and faults at a radial distance of ~5.5–6.0 km from the crater center (see Fig. 4 for location). Solid and dashed lines represent faults and bedding surfaces, respectively. Sub-vertical uplifted strata (right of image) are juxtaposed against shallow-dipping strata (left of image). The latter contain several bedding-parallel detachment faults that record evidence for outward-directed movement of hanging-wall blocks (displacement ~2–7 m). These detachment faults are cut by the sub-vertical concentric faults on the right of this image. UTM 420,800 m.E. 8,362,000 m.N.

upwards, creating a converging particle trajectory field (e.g., Wilshire and Howard 1968; Wilson and Stearns 1968; Offield and Pohn 1972; Milton et al. 1996a). Gravitational collapse of over-heightened or unstable central uplifts may also occur in larger complex impact structures resulting in a subsequent phase of outward and downward movement (e.g., Collins et al. 2002; Wieland et al. 2003). Further complexity is suggested by the results of laboratory experiments and computer simulations, which reveal that uplift of the transient cavity floor may commence before outward growth and excavation of the transient cavity ceases (Gault et al. 1968; Stöffler et al. 1975; Orphal 1977; Schultz et al. 1981; Kenkmann et al. 2000).

There can be no argument that Haughton has a central uplift. Large, kilometer-size fault-bounded blocks of the Eleanor River Formation and smaller (up to ~50–150 m across) blocks of the Blanley Bay Formation have been uplifted >1050 to <1300 m and >1300 to <1450 m, respectively, above their pre-impact stratigraphic positions (Fig. 1; map insert). However, what remains to be determined is the nature and extent of the central uplift at Haughton. Several workers have preferred to use the generic term “central uplift” (Frisch and Thorsteinsson 1978; Bischoff and Oskierski 1988; Grieve 1988). An early suggestion that Haughton was transitional between a peak ring and a multi-ring basin (Robertson and Sweeney 1983) has been discounted (Bischoff and Oskierski 1988). Recently, in a series of abstracts, Sharpton and co-workers have suggested that Haughton is a peak ring structure (Sharpton et al. 1998; Sharpton 1999; Sharpton and Dressler 2003).

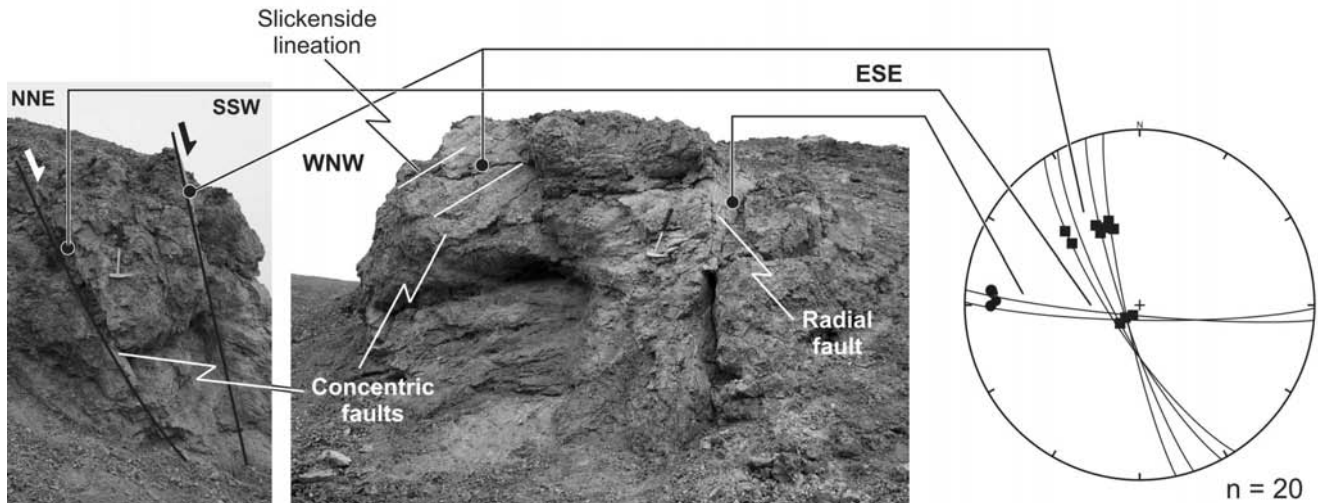


Fig. 14. A field photograph of concentric and radial faults from sector 5 (see Fig. 4 for location). Slickenside lineations from fault surfaces are plotted on an equal-angle stereonet. In this method, vertical lineations will plot at the center of the stereonet, while horizontal lineations will plot on the circumference. Circles represent data from radial faults and squares from concentric faults. UTM 417,750 m.E. 8,368,430 m.N.

It has been noted for some time that Haughton does not possess a central peak, as summarized most recently by Grieve and Therriault (2004). This is confirmed by the present structural study. Furthermore, several lines of evidence suggest that the central uplift was completely covered with impact melt breccias in the newly formed Haughton crater. In particular, impact melt breccias would have originally filled the central ~12 km diameter central region of Haughton (Osinski et al. 2005b). Given that such lithologies presently occur at elevations of up to ~220 m above sea level, >25–60 m above the highest elevation of the Eleanor River Formation outcrops, this suggests that the latter were originally completely buried. The presence of lake sediments of the Haughton Formation at lower elevations than the Eleanor River Formation cannot be used as evidence for a topographic peak (e.g., Sharpton 1998; Sharpton and Dressler 1999), as new field studies reveal that a substantial amount of erosion of impact melt breccias occurred before deposition of the Haughton Formation (Osinski and Lee 2005). There is, therefore, no central peak or peak ring at Haughton, as the original definitions of these features require that they emerge through the crater-fill deposits (Grieve et al. 1981).

Haughton does not stand alone in lacking a central topographic peak (cf. Grieve and Pilkington 1996; Grieve and Therriault 2004). So, too, does the similarly sized Ries impact structure, Germany (Pohl et al. 1977). It is interesting to note, however, that the ~25 km diameter Boltysh impact structure, Ukraine, does possess a central peak that is emergent through the crater-fill deposits (Masaitis 1999). This could suggest that the lack of a central peak is due to the presence of a thick sedimentary cover sequence at Haughton (~1880 m) and the Ries (~500–850 m), whereas Boltysh formed in an entirely crystalline target. However, other impact characteristics (e.g.,

projectile density, impact velocity, and so forth) may also be involved (see discussion in Grieve and Therriault 2004).

New mapping reveals that the central uplift at Haughton comprises three discrete structural zones. The central region, ~2 km in diameter, is interpreted to represent a core of isolated, differentially uplifted megablocks of variable orientation. This core correlates with a central positive magnetic anomaly of 300–500 nT (Glass et al. 2005) and a negative gravity anomaly of ~3 mgal (Pohl et al. 1988). Surrounding the central core of megabreccia are several large kilometer-size fault-bounded blocks of Eleanor River Formation that generally display dips of ~10–40°. These lithologies have been uplifted >950 to <1200 m above their pre-impact stratigraphic position. Overlying the uplifted blocks of Eleanor River Formation are several gently dipping (up to ~30°) “plates” of Bay Fiord Formation strata. Kinematic indicators indicate that the latter were transported inward and upwards, and thrust over the underlying units of Eleanor River Formation, removing up to ~300 m of the stratigraphic section in places. Evidence for later, minor, extensional collapse outward from the center of the uplift is also present. Thus, there was a switch from inward and upward movement during initial uplift, to outward and downward movement during subsequent collapse of the unstable central uplift (cf. the Vredefort impact structure, South Africa [Wieland et al. 2003]). It is interesting to note that comparable kinematics are predicted by the numerical models of crater collapse and peak ring formation by Collins et al. (2002). We will return to this below.

A similar arrangement of a central core of megabreccia surrounded by a zone of more coherent, relatively flat lying units, occurs at many other impact structures developed in sedimentary targets (e.g., Decaturville [Offield and Pohl 1972], Red Wing Creek [Brenan et al. 1975], Wells Creek

[Wilson and Stearns 1968], USA). Drilling at Decaturville also suggests that the megabreccia is of limited lateral extent and confined underneath beds that have slid inward and upward (Offield and Pohn 1977). This is consistent with the present-day surface expression at Haughton.

A zone of (sub-) vertical and/or overturned strata occurs at Haughton at a radial distance from the center of ~5.0–6.5 km. These lithologies are highly fractured and faulted and are uplifted by >250 to <850 m. This zone comprises a series of discrete, fault-bounded sheets or blocks, with major changes of orientation evident across many faults (cf. Gosses Bluff [Milton et al. 1996a]). This study reveals that this zone is more or less continuous around the Haughton structure, in contrast to earlier findings (Robertson and Sweeney 1983; Bischoff and Oskierski 1988). There are two main possible origins for this zone of (sub-) vertical and/or overturned strata and faults at Haughton. In the first scenario, this zone represents complex interactions between an outward collapsing central uplift and inward collapsing crater walls. In this model, this region represents the outer edge of the central uplift. The other possibility is that this zone represents the remains of the uplifted and overturned rim of the transient cavity. Importantly, well-developed shatter cones are present in this zone indicating shock pressures of >2 GPa (Roddy and Davis 1977). Such high shock pressures are unlikely to have occurred in a transient cavity rim, but are consistent with this zone representing the outer edge of the central uplift. This is supported by kinematic evidence, which reveals that these lithologies originally moved inward, with later outward-directed displacement. This is consistent with the formation and subsequent partial collapse of an over-heightened or unstable central uplift. For a transient cavity rim, the opposite kinematic history is more likely (i.e., outward movement during transient cavity growth, followed by inward displacement during subsequent collapse).

Thus, the evidence suggests that this structurally complicated region at Haughton represents the interference zone between the outward collapsing central uplift and inward collapsing crater walls (cf. numerical models of Collins et al. 2002). If this interpretation is correct, it may help to explain the lack of a central peak or peak ring at Haughton. That is, a “peak” may have formed early on during the modification stage, but subsequently collapsed during the final stages of crater formation. However, this collapse was not sufficient enough for a peak ring to form. This is consistent with the smaller transient cavity at Haughton (~12 km diameter) compared to the simulations of Collins et al. (2002), which modeled the collapse of a transient cavity 100 km in diameter.

Bischoff and Oskierski (1988) have suggested that parts of this ring-like zone at a radial distance from the crater center of ~5.0–6.5 km at Haughton resemble the so-called “inner ring” of the Ries structure (Pohl et al. 1977). While this may be so, there are important differences. In particular, the inner

ring at Ries conforms to all the definitions of a peak ring (i.e., a semi-continuous ring of hills that originally protruded through the crater-fill deposits in the fresh crater) (Grieve et al. 1981). As noted above, the ring-like zone at Haughton is not a peak ring. These ring-like structures at Haughton and Ries are, however, structurally very similar. At Haughton, this zone comprises uplifted, rotated, and often overturned units that are heavily fractured and faulted. At the Ries structure, it is harder to unravel the tectonic history of the inner ring, as it predominantly comprises heavily faulted and fractured crystalline lithologies. However, shallow drilling within the inner ring reveals that crystalline rocks commonly overlie sedimentary rocks, indicating an inverted stratigraphic sequence (Pohl et al. 1977). These similarities may suggest that the ring-like structures at Haughton and Ries share a common origin. In this scenario, the presence of a thick sequence of sedimentary target rocks and/or differences in impact parameters, presumably subdued the formation of a topographic peak ring at Haughton.

Tectonics of Crater Rim Collapse

The collapse of the transient cavity walls results in inward movement of rock masses and a converging particle trajectory field. It is generally believed that this displacement takes place along curved or listric fault surfaces that dip in toward the crater center (e.g., Spray 1997; Melosh and Ivanov 1999; Kenkmann and von Dalwigk 2000). During this inward collapse, space problems arise as displaced rock masses are forced into a smaller and smaller area. This is overcome by bulk thickening of target material by folding, repetition along thrust faults, and other forms of radial transpression ridges (Kenkmann and von Dalwigk 2000).

This work reveals that the collapse of the crater walls in the early-formed Haughton crater involved the complex interaction of a series of interconnected concentric and radial faults. It is noticeable that the intensity and style of concentric faulting changes around the periphery of the crater, resulting in a distinct asymmetric structural pattern (cf. Bischoff and Oskierski 1988). The kinematics of crater rim collapse at Haughton will now be described in detail and synthesized with results from other impact sites.

Concentric Faulting

Arcuate, concentric-oriented faults have been observed at all complex craters where sufficient exposures and/or geophysical data exists. Concentric faults with strike lengths of several kilometers have been mapped out at Haughton to a radial distance of 12 km to the north, west, and south, and 11 km to the east. This gives an apparent crater diameter of 23 km for Haughton, using the terminology of Grieve et al. (1981) (i.e., this does not represent the rim [final crater] diameter). Concentric faults are predominantly listric extensional faults with rotation of beds in the hanging-wall up

to $\sim 75^\circ$. The outermost concentric faults dip in toward the center of the crater, with rollover anticlines present in the hanging-walls of some of the larger examples. These features are common in terrains dominated by extensional tectonics, such as the Basin and Range structure of the Great Basin of California, Nevada, and Utah (e.g., Stewart 1972). The presence of such structures at Haughton is not surprising and is consistent with the inward collapse of the transient cavity walls.

It is apparent from this study that, in general, the innermost concentric faults tend to dip away from the crater center. This accounts for the curious inward dip of the sedimentary formations in some regions of the crater noted by previous workers (Bischoff and Oskierski 1988). Importantly, the distribution of outward-dipping faults is markedly asymmetric around the Haughton structure. They are abundant out to radial distances of ~ 8 km in the southern and southwestern regions (sectors 4 and 5) (Fig. 4). In contrast, outward-dipping faults appear to be absent or poorly developed in the northwest (sector 6) and present out to radial distances of only ~ 5 km in the north and eastern regions (sectors 2 and 3). This explains the lack of outward-dipping faults on the seismic section through sector 6 (Fig. 3) (Scott and Hajnal 1988). However, it is important to note that the presence of such faults was not predicted by cratering models at the time of the seismic studies, so they may have been missed. It is, therefore, notable that several uncorrelated inward-dipping seismic reflectors are seen in Fig. 3 that may represent rotated bedding reflectors due to displacement along outward-dipping listric faults.

What is the origin of these outward-dipping listric faults? One possibility is that these structures represent "antithetic faults." Antithetic faults dip in the opposite direction to major listric faults and eliminate the gaps that would otherwise be produced by displacements on curved surfaces (e.g., Davis and Reynolds 1996). Such faults, along with crestal collapse grabens and rollover anticlines, are ubiquitous in extensional terrains where listric faulting predominates (e.g., Stewart 1972; Wernicke and Burchfield 1982; Ellis and McClay 1988). The presence of such features at Haughton suggests, therefore, that some of the outward-dipping faults are antithetic faults that formed as a consequence of the collapse of the transient cavity walls along major, inward-dipping listric faults.

The above explanation does not fully account for the outward-dipping faults being concentrated nearest to the central uplift, and inward-dipping faults predominating at the crater periphery. The most obvious explanation for this phenomenon is that the central uplift itself played an important role in governing the nature of faulting during crater rim collapse. Importantly, in some places (e.g., sectors 4 and 5) (Fig. 4), outward-dipping faults are developed in lithologies that are uplifted above their pre-impact stratigraphic position, around the edge of the central uplift. In

other words, although these lithologies have been down-faulted along outward-dipping listric faults, they are still uplifted (i.e., they must have originally been uplifted by greater amounts). Thus, a second mechanism for the formation of these outward-dipping listric faults at Haughton is that they were formed during outward collapse of the outer edges of the central uplift.

The outermost concentric faults at Haughton typically display two episodes of deformation: (1) early major dip-slip extensional movement; and (2) later minor oblique strike-slip movement. Importantly, this oblique strike-slip movement has resulted in the offset of many radial faults, indicating a temporal relationship between the two styles of faulting. Thus, centripetal (i.e., concentric or circular) motions were important in accommodating strain during collapse of the transient cavity walls at Haughton.

Detachment Faults

Sub-horizontal, bedding-parallel detachment faults have been observed in the crater rim region at Haughton, particularly in south. Two lines of evidence suggest that these features developed during the outward growth of the transient cavity during the excavation stage of crater formation. Firstly, kinematic indicators record evidence for outward-directed movement of the hanging-wall blocks. Secondly, tectonic features developed during the inward collapse of the crater walls overprint the detachment faults. Sub-horizontal detachment faults have also recently been documented inside and beyond the crater rim of the Ries impact structure by Kenkmann and Ivanov (2005). These authors provided field evidence and numerical models, which suggest that detachment faults form in the target rocks surrounding transient cavities in response to spallation and subsequent shearing during ejecta curtain drag during the excavation stage of complex crater formation, findings that are supported by the field evidence at Haughton.

Radial Faulting

Faults, fractures, and other features such as impact melt dykes, with radial orientations, are common in terrestrial impact structures. While it is apparent that radial structures are important in accommodating the collapse of complex craters (e.g., Kenkmann and von Dalwigk 2000), little attention has been paid to the timing and inception mechanisms of such features.

Three major categories of radial faults have been observed at Haughton:

1. Sub-vertical oblique strike-slip faults that record little (< 10 m) or no displacement of marker beds. This is despite the fact that substantial volumes of fault breccia (> 8 m) are typically present. Thus, these faults have accommodated substantial back-and-forth movement, but very little overall displacement. Importantly, the majority of these radial faults are cut and offset by

concentric faults, providing a temporal relationship between the two styles of faulting. It is, therefore, suggested that these radial faults were formed early on in the crater-forming process during the outward growth of the transient cavity (i.e., during the excavation stage). This is consistent with recent work on so-called offset dikes at Sudbury, which indicate that radial faults/fractures are generated very early in the impact process and that they precede the concentric faults as well as melt sheet formation (Murphy and Spray 2002).

2. Steeply dipping (>70°) oblique strike-slip faults with considerable displacement. These faults accommodated the transfer of deformation between inward sliding masses due to inward collapse of the transient cavity walls along concentric listric faults. This style of radial faulting resulted in the development of positive flower structures and other radial transpression ridges at Haughton (cf. Siljan impact structure [Kenkmann and von Dalwigk 2000]). Radial faults with predominantly (oblique) strike-slip movements have been mapped at several other impact sites (e.g., the Decaturville [Offield and Pohn 1972, 1977], and Siljan [Kenkmann and von Dalwigk 2000] impact structures in the USA and Sweden, respectively).
3. Listric normal radial faults that were only observed in the southwest of the Haughton structure. This is unexpected and suggests that, in this region, tensional stresses were acting during crater collapse. The structures produced resemble the so-called radial transtension troughs of Kenkmann and von Dalwigk (2000), although at Haughton these structures occur in the crater rim region and not the central uplift as in the model of Kenkmann and von Dalwigk (2000).

Folding

Folds are a minor but ubiquitous feature of the Haughton structure. As noted above, anticlines are present in the hanging-walls of several of the largest listric extensional faults. These folds are a common manifestation of extensional tectonics and develop due to space problems created by inward movement along curved fault surfaces. Radially oriented folds are also present at Haughton. These signify bulk thickening of inward sliding masses during collapse of the transient cavity walls (cf. Kenkmann and von Dalwigk 2000). Radial and concentric folds occur in many other impact structures developed in sedimentary targets (e.g., the Decaturville [Offield and Pohn 1972], Sierra Madera [Wilshire et al. 1972], and Wells Creek [Wilson and Stearns 1968] impact structures), but apparently not in structures formed in crystalline targets (Lana et al. 2003).

The occurrence of folding during the Haughton impact event does not indicate ductile deformation. On the contrary, folding was accommodated along localized, small-scale brittle (micro-) faults, in agreement with studies from other terrestrial impact sites (e.g., Kenkmann 2002).

Target Weakening and Strength Degradation

It is clear that to account for the observed dependence of final crater morphology on crater diameter, the target rocks surrounding a crater must be weakened in some way (Melosh and Ivanov 1999). Melosh (1977) suggested that transient cavity collapse occurs in a material that behaves as a Bingham fluid with a yield stress of ~30 bars, accompanied by an effective internal angle of friction <5° (McKinnon 1978). However, there are major differences between the behavior of a Bingham fluid and the static rheology of rocks (Jaeger and Cook 1969). Thus, a mechanism whereby the rocks are temporarily fluidized is required. The most commonly proposed mechanism is that of “acoustic fluidization” (Melosh 1979). In this model, strong shaking caused by the passage of acoustic waves through “fragmented rock debris” temporarily reduces the overburden pressure, allowing fluidization to occur on the macroscopic scale. A fundamental assumption of the acoustic fluidization model is that the target rocks deform as a continuum and that the lengths of the elastic waves are larger than any intact rock fragments (Melosh 1979).

The original acoustic fluidization theory was later modified to form the “block model” (Ivanov and Kostuchenko 1997; Melosh and Ivanov 1999). This model was based on preliminary observations from drilling at the ~40 km diameter Putschev-Katunki impact structure, Russia, in which the central uplift is apparently composed of a series of blocks ranging in size from ~50 to 200 m across (Ivanov et al. 1996). There are some important parameters that must be met for the block oscillation model to be valid. In particular, “the sound speed of the matrix between blocks must be much smaller than that of the intact rock” (Melosh and Ivanov 1999). In other words, for the block oscillation model to be applicable, the inter-block matrix should comprise a soft layer of breccia ~10–20% of the block’s thickness (i.e., ~10–20 m of breccia for a block ~100 m across, or 100–200 m of breccia for a 1 km size block). Thus, the two acoustic fluidization models can be thought of as two end members, with the target either deforming as a continuum (original model of Melosh 1979) or as a series of blocks (block model of Ivanov and Kostuchenko 1997).

It is clear that rocks do not deform as a ductile metal-like continuum, but as a series of discrete blocks (e.g., Melosh and Ivanov 1999). This is apparent with respect to the central uplift at Haughton, a feature that is common for many terrestrial impact structures developed in predominantly sedimentary targets (e.g., Decaturville, Gosses Bluff, Sierra Madera, Wells Creek). Seismic reflection studies at Haughton also indicate a loss of coherent reflections and a decrease in seismic velocity in the central uplift (Scott and Hajnal 1988). These observations are broadly consistent with the block oscillation model of acoustic fluidization. However, at Haughton, apart from the central ~1–2 km diameter core of megabreccia, the blocks are several hundred meters to

kilometers in size, requiring inter-block breccias >50–100 m thick. No evidence for such volumes of breccia is seen in the field. Instead, deformation in the central uplift at Haughton, at least in the near-surface region, was predominantly accommodated along discrete faults, associated with up to a few meters of breccia, and along numerous millimeter- to centimeter-size crush zones and cataclases within the blocks. Brecciation and intense fracturing of entire outcrops does occur, but is spatially limited. It is not clear whether the combined action of faulting, pervasive fracturing, and limited wholesale brecciation of the target rocks, could have provided the necessary strength degradation to allow the formation of the central uplift at Haughton. However, it is apparent that if acoustic fluidization did play a role in reducing the strength of the target lithologies during central uplift formation at Haughton, it was likely to have been via a combination of the original continuum theory of Melosh (1979), and the modified block model of Ivanov and Kostuchenko (1997).

Kinematic Model for Complex Crater Formation

The Haughton impact structure is one of the best preserved and best exposed mid-size terrestrial impact structures (e.g., ~15–30 km) and is the only structure of this size to have been completely mapped in detail. Based on our structural studies of Haughton and a review of the existing literature, we present the following kinematic model of complex crater formation (Fig. 15). While this model is by no means definitive, we hope that it will provide constraints for numerical models and drive further field studies of other terrestrial impact structures.

The formation of hypervelocity impact craters has been divided, somewhat arbitrarily, into three main stages (e.g., Gault et al. 1968): (1) contact and compression; (2) excavation; and (3) modification. It is widely accepted that the morphological diversity of impact craters “is not a direct result of the crater excavation process but develops only after most of the material has been expelled from the crater” (Melosh and Ivanov 1999). In other words, the final form of a crater is assumed to be the result of processes acting during the modification stage of crater formation.

A key concept in the formation of hypervelocity impact craters is the so-called “transient cavity.” This theoretical construct represents the initial product of crater excavation and is formed as the roughly hemispherical shock wave propagates out into the target sequence (Dence 1968; Grieve and Cintala 1981). This transient cavity then “undergoes different degrees of modification as a result of gravitational instability and collapse” (Melosh and Ivanov 1999). For crater diameters <2–4 km on Earth, the transient cavity undergoes only minor modification resulting in the formation of a simple bowl-shaped crater. However, above a certain size threshold (>2–4 km diameter), substantial modification of the transient cavity occurs, producing a so-called complex impact crater (Dence 1965).

It has been acknowledged for some time that pre-existing structures in the target rocks (e.g., faults, joints, etc.) can exert considerable influence on the geometry of the transient cavity as evidenced by the squarish outline of Meteor Crater (Shoemaker and Kieffer 1974). However, an important finding of our studies of Haughton is that new structures are also generated during the initial compressive outward-directed growth of the transient cavity during the excavation stage of crater formation (Fig. 15a): (1) sub-vertical radial faults and fractures; (2) sub-horizontal bedding parallel detachment faults (cf. the Ries structure [Kenkmann and Ivanov 2005]); and (3) minor concentric faults and fractures. While we agree that the morphological diversity of impact craters “is not a direct result of the crater excavation process” (Melosh and Ivanov 1999), we suggest that structures generated during this stage may play an important role during the subsequent modification stage, including reducing the overall strength of the target sequence prior to crater collapse. Evidence for fracture development and breccia emplacement during transient cavity formation has also been described from the Chicxulub impact structure, Mexico (Wittmann et al. 2003).

Toward the end of the excavation stage, uplift of the transient cavity floor occurs resulting in the formation of a central uplift (Fig. 15b). Material originally displaced downward and outward in the floor of the transient cavity is transported inward and upward, creating a converging particle trajectory field in the center of the crater (Fig. 15b). This compressional inward-directed deformation results in the duplication of strata along thrust faults and folds. At the very center of many small to mid-size complex impact structures, this deformation typically reduces uplifted lithologies to a megabreccia of isolated, differentially uplifted, megablocks, confined beneath large kilometer-scale coherent blocks bounded by thrust faults. However, it is evident that the overall stratigraphy is preserved within this megabreccia core (i.e., the oldest, deeper lithologies occur in the center, surrounded by lithologies derived from progressively shallower levels in the pre-impact target sequence).

Shortly thereafter, the transient cavity reaches its maximum radial extent, which marks the end of the excavation stage (Fig. 15c). Subsequently, the initially steep walls of the transient cavity collapse under gravitational forces (Fig. 15d). This induces an inward and downward movement of large (~100 m to km scale) fault-bounded blocks along a series of interconnected radial and concentric faults (Fig. 15d). It is widely assumed that these faults form in the late stages of an impact event; however, as discussed above, it appears that some of these radial and concentric faults are generated during the excavation stage and subsequently re-activated during the modification stage.

The bulk of the displacement during collapse of transient cavity walls occurs along inward-dipping listric extensional faults (Fig. 15d) (e.g., Spray 1997; Melosh and Ivanov 1999). However, it is apparent that outward-dipping concentric faults

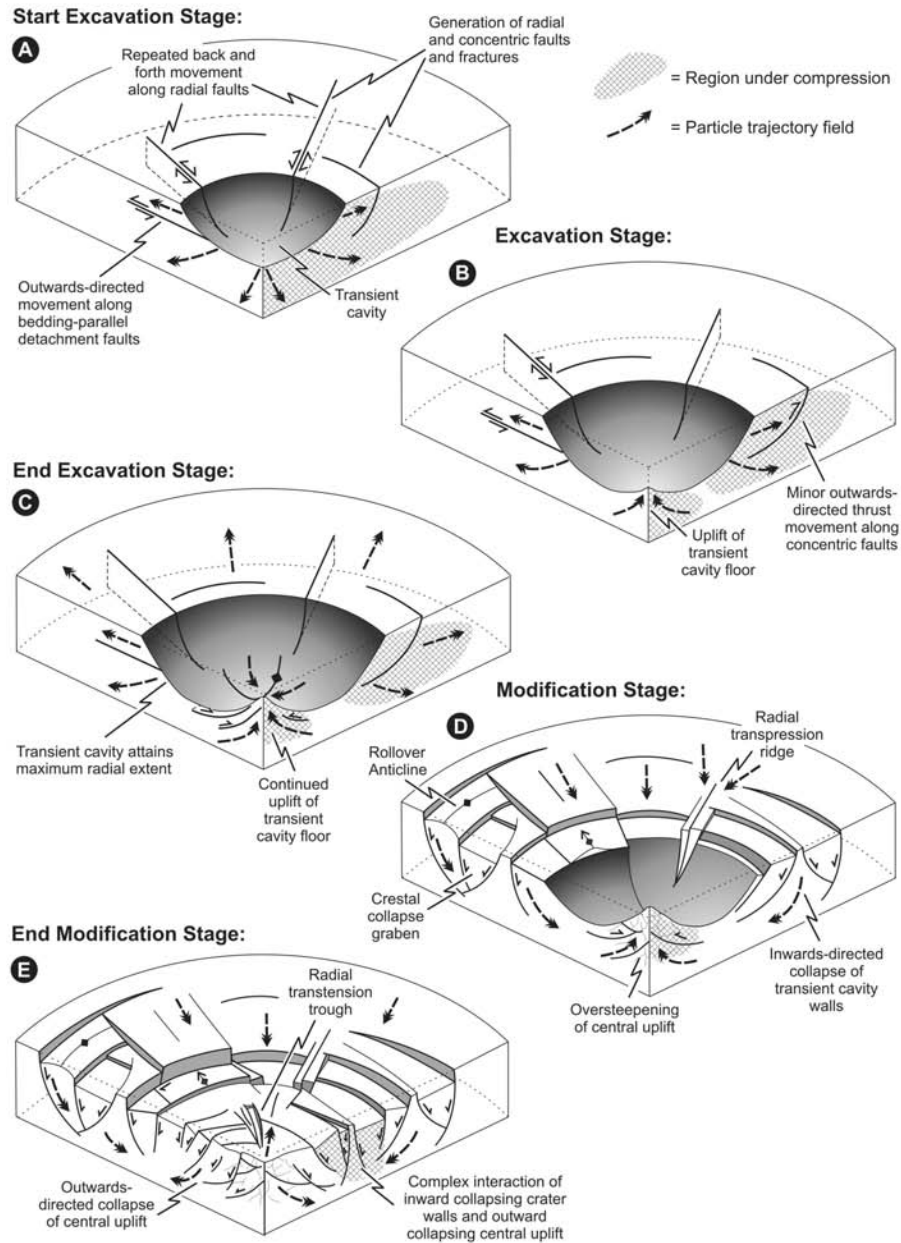


Fig. 15. A series of schematic diagrams showing the formation of a generic mid-size complex impact crater. The first stage of an impact event begins when the projectile, be it an asteroid or comet, contacts the surface of the target (not shown). During the excavation stage (a), roughly hemispherical shock waves propagate out into the target sequence. Shock waves that initially travel upwards intersect the ground surface and generate rarefaction waves that propagate back downward into the target sequence (Melosh 1989). The combination of the outward-directed shock waves and downward-directed rarefaction waves produces an “excavation flow” and generates a so-called transient cavity (Dence 1968; Grieve and Cintala 1981). Several new structures are generated in the floor and walls of the expanding transient cavity during this initial compressive outward-directed deformation. At some point during the excavation stage, the transient cavity attains its maximum depth. Subsequently, uplift of the transient cavity floor occurs resulting in the formation of a central uplift (b). Eventually, a point is reached at which the shock and rarefaction waves can no longer excavate or displace target rock and melt (French 1998). At this point, the transient cavity attains its maximum radial extent, which marks the end of the excavation stage (c). During the subsequent modification stage, continued uplift of the transient cavity floor occurs (d). In addition, the walls of the transient cavity collapse inward along a series of interconnected radial and concentric faults. These faults represent a combination of reactivated structures formed during the excavation stage, and new structures formed during the modification stage. Toward the end of the modification stage, the central uplift can become over-heightened or unstable (e). Complex interactions between the outward collapsing central uplift and inward collapsing crater walls produces a structurally complex zone of highly faulted, uplifted, sub-vertical faults and strata around the margin of the central uplift. See text for further explanation.

are an important structural feature of Haughton and, by analogy, other complex impact craters, although lack of exposure at the majority of terrestrial impact sites hampers their determination (Fig. 15d). It is apparent that these outward-dipping concentric faults formed through a combination of two processes. Some represent antithetic faults formed in response to inward collapse of the transient cavity walls. Others, especially those around the outer edge of the central uplift, likely formed due to outward collapse of the uplift itself. As evidenced by detailed mapping at Haughton, deformation during collapse of transient cavity walls can be asymmetric. For example, in the north and east of the Haughton structure, the bulk of the displacement occurred along a major, >20 km long inward-dipping listric fault. In the southern sector, the majority of concentric faults dip outward from the crater center with only the very outermost faults dipping in toward the crater center. There is also a reduction in the length of concentric faults in this zone. The southwestern sector is structurally very complicated and in places, deformation is seemingly chaotic. In contrast, the northwestern sector appears to have acted as a relatively stable block, with little overall displacement along concentric faults. Field and seismic studies (Scott and Hajnal 1988) also indicate that the inward-dipping concentric faults do not link into a basal detachment fault as suggested by Kenkmann and von Dalwigk (2000), except in the innermost parts of the crater rim.

Converging particle flow during crater collapse at Haughton and other craters is accommodated via several tectonic features (Fig. 15d): (1) sub-vertical radial faults and folds, which result in the formation of radial transpression ridges, such as positive flower structures and chaotically brecciated ridges (Kenkmann and von Dalwigk 2000); (2) outward-dipping antithetic concentric faults; (3) crestal collapse grabens and rollover anticlines, formed in response to the interaction of outward- and inward-dipping concentric faults; and (4) late-stage oblique strike-slip movement along concentric faults, suggesting that centripetal (i.e., concentric or circular) motions are also important in accommodating strain during collapse of the transient cavity walls.

Field evidence from the Vredefort impact structure (Wieland et al. 2003) and numerical models of large impact events (Collins et al. 2002) suggest that central uplifts can become over-heightened or unstable and so undergo gravitational collapse resulting in a subsequent phase of extensional, outward-directed movement. In the models of Collins et al. (2002), the outer edges of the collapsed central uplift are thrust over the inward collapsing crater walls, resulting in the formation of peak rings. Importantly, at Haughton, there is kinematic evidence for minor, extensional collapse of the central uplift and complex interactions between this outward-directed material and the inward collapsing crater walls (Fig. 15e). We suggest that this collapse resulted in the destruction of an early-formed central

peak, but, due to the smaller size of the Haughton transient cavity, collapse ended before a peak ring could be formed (cf. the numerical models of Collins et al. 2002). However, given that a peak ring is present at the similarly sized Ries impact structure, either the presence of a thick sedimentary cover at Haughton or differences in the impact parameters limited central uplift collapse and peak ring formation.

Acknowledgments—Data collection for this study was carried out while G.R.O. was a Ph.D. student at the University of New Brunswick and was funded by the Natural Sciences and Engineering Research Council of Canada (NSERC) through research grants to J.G.S. G.R.O. is currently funded by an NSERC Visiting Fellowship in Canadian Government Laboratories at the Canadian Space Agency (CSA). We thank Pauline and Rhoda Akeagok, Joe Amarualik, Alain Berinstain, A. C. Hitch, “Kimmig,” Colleen Lenahan, Samson Ootoovak, John Schutt, and Nesha Trenholm; along with everyone involved in the Haughton-Mars Project for assistance during the HMP 1997–2004 field seasons. Additional field support was provided by the Polar Continental Shelf Project (Natural Resources Canada), the Nunavut Research Institute, and the communities of Grise Fiord and Resolute Bay. We are grateful to Richard Grieve and Boris Ivanov for their detailed and constructive reviews. PASSC publication number 41. This is contribution HMPSCI 2004-003.

Editorial Handling—Dr. Richard Grieve

REFERENCES

- Bischoff L. and Oskierski W. 1988. The surface structure of the Haughton impact crater, Devon Island, Canada. *Meteoritics* 23: 209–220.
- Chao E. C. T., Hüttner R., and Schmidt-Kaler H. 1978. *Principal exposures of the Ries meteorite crater in southern Germany*. Munich: Bayerisches Geologisches Landesamt. 84 p.
- Collins G. S., Melosh H. J., Morgan J. V., and Warner M. R. 2002. Hydrocode simulations of Chicxulub crater collapse and peak-ring formation. *Icarus* 157:24–33.
- Davis G. H. and Reynolds S. J. 1996. *Structural geology of rocks and regions*, 2nd ed. New York: John Wiley & Sons. 776 p.
- Dawes P. R. and Christie R. L. 1991. Geomorphic regions. In *Geology of the Innuitian Orogen and Arctic Platform of Canada and Greenland, geological survey of Canada, geology of Canada 3*, edited by Trettin H. P. Ottawa: Geological Survey of Canada. pp. 29–56.
- Dence M. R. 1964. A comparative structural and petrographic study of probable Canadian meteorite craters. *Meteoritics* 2:249–270.
- Dence M. R. 1965. The extraterrestrial origin of Canadian craters. *Annals of the New York Academy of Science* 123:941–969.
- Dence M. R. 1968. Shock zoning at Canadian craters: Petrography and structural implications. In *Shock metamorphism of natural materials*, edited by French B. M. and Short N. M. Baltimore: Mono Book Corp. pp. 169–184.
- Ellis P. G. and McClay K. R. 1988. Listric extension fault systems: Results of analogue model experiments. *Basin Research* 1:55–70.

- French B. M. 1998. *Traces of catastrophe: A handbook of shock-metamorphic effects in terrestrial meteorite impact structures*. LPI Contribution #954. Houston: Lunar and Planetary Institute. 120 p.
- Frisch T. and Thorsteinsson R. 1978. Haughton astrobleme: A mid-Cenozoic impact crater, Devon Island, Canadian Arctic Archipelago. *Arctic* 31:108–124.
- Gault D. E., Quaide W. L., and Oberbeck V. R. 1968. Impact cratering mechanics and structures. In *Shock metamorphism of natural materials*, edited by French B. M. and Short N. M. Baltimore: Mono Book Corp. pp. 87–99.
- Glass B. J., Domville S., and Lee P. 2005. Further geophysical studies of the Haughton impact structure (abstract #2398). 36th Lunar and Planetary Science Conference. CD-ROM.
- Grieve R. A. F. 1988. The Haughton impact structure: Summary and synthesis of the results of the HISS project. *Meteoritics* 23:249–254.
- Grieve R. A. F. and Cintala M. J. 1981. A method for estimating the initial impact conditions of terrestrial cratering events, exemplified by its application to Brent Crater, Ontario. Proceedings, 12th Lunar and Planetary Science Conference. pp. 1607–1621.
- Grieve R. A. F. and Pilkington M. 1996. The signature of terrestrial impacts. *Journal of Australian Geology and Geophysics* 16:399–420.
- Grieve R. A. F. and Therriault A. 2004. Observations at terrestrial impact structures: Their utility in constraining crater formation. *Meteoritics & Planetary Science* 39:199–216.
- Grieve R. A. F., Robertson P. B., and Dence M. R. 1981. Constraints on the formation of ring impact structures, based on terrestrial data. In *Proceedings of the conference on multi-ring basins: Formation and evolution*, edited by Schultz P. H. and Merrill R. B. New York: Pergamon Press. pp. 37–57.
- Hajnal Z., Scott D., and Robertson P. B. 1988. Reflection study of the Haughton impact crater. *Journal of Geophysical Research* 93: 11,930–11,942.
- Hickey L. J., Johnson K. R., and Dawson M. R. 1988. The stratigraphy, sedimentology, and fossils of the Haughton Formation: A post-impact crater-fill, Devon Island, N.W.T., Canada. *Meteoritics* 23:221–231.
- Ivanov B. A., Kocharyan G. G., Kostuchenko V. N., Kirjakov A. F., and Pevzner L. A. 1996. Puchezh-Katunki impact crater: Preliminary data on recovered core block structure (abstract). 27th Lunar and Planetary Science Conference. pp. 589–590.
- Ivanov B. A. and Kostuchenko V. N. 1997. Block oscillation model for impact crater collapse (abstract #1655). 28th Lunar and Planetary Science Conference. CD-ROM.
- Jaeger J. C. and Cook N. G. W. 1969. *Fundamentals of rock mechanics*. London: Chapman & Hall. 515 p.
- Jessberger E. K. 1988. ⁴⁰Ar–³⁹Ar dating of the Haughton impact structure. *Meteoritics* 23:233–234.
- Kenkmann T. 2002. Folding within seconds. *Geology* 30:231–234.
- Kenkmann T. and von Dalwigk I. 2000. Radial transpression ridges: A new structural feature of complex impact craters. *Meteoritics & Planetary Science* 35:1189–1201.
- Kenkmann T. and Ivanov B. 2005. Thin-skin delamination of target rocks around the Ries Crater: The effect of spallation and ejecta drag (abstract #1039). 36th Lunar and Planetary Science Conference. CD-ROM.
- Kenkmann T., Ivanov B. A., and Stöffler D. 2000. Identification of ancient impact structures: Low-angle faults and related geological features of crater basements. In *Impacts and the early Earth*, edited by Gilmour I. and Koeberl C. Berlin: Springer-Verlag. pp. 279–307.
- Kriens B. J., Shoemaker E. M., and Herkenhoff K. E. 1999. Geology of the Upheaval Dome impact structure, southeast Utah. *Journal of Geophysical Research* 104:18,867–18,887.
- Lana C., Gibson R. L., and Reimold W. U. 2003. Impact tectonics in the core of the Vredefort dome, South Africa: Implications for central uplift formation in very large impact structures. *Meteoritics & Planetary Science* 38:1093–1107.
- Masaitis V. L. 1999. Impact structures of northeastern Eurasia: The territories of Russia and adjacent countries. *Meteoritics & Planetary Science* 34:691–711.
- McKinnon W. B. 1978. An investigation into the role of plastic failure in crater modification. Proceedings, 9th Lunar and Planetary Science Conference. pp. 3965–3973.
- Melosh H. J. 1977. Crater modification by gravity: A mechanical analysis of slumping. In *Impact and explosion cratering*, edited by Roddy D. J., Pepin R. O., and Merrill R. B. New York: Pergamon Press. pp. 1245–1260.
- Melosh H. J. 1979. Acoustic fluidization: A new geologic process? *Journal of Geophysical Research* 84:7513–7520.
- Melosh H. J. 1989. *Impact cratering: A geologic process*. New York: Oxford University Press. 245 p.
- Melosh H. J. and Ivanov B. A. 1999. Impact crater collapse. *Annual Review of Earth and Planetary Science* 27:385–415.
- Milton D. J., Barlow B. C., Brown A. R., Moss F. J., Manwaring E. A., Sedmik E. C. E., Young G. A., and Van Son J. 1996a. Gosses Bluff—A latest Jurassic impact structure, central Australia. Part 2: Seismic, magnetic, and gravity studies. *Journal of Australian Geology and Geophysics* 16:487–527.
- Milton D. J., Glikson A. Y., and Brett R. 1996b. Gosses Bluff—A latest Jurassic impact structure, central Australia. Part 1: geological structure, stratigraphy, and origin. *Journal of Australian Geology and Geophysics* 16:453–486.
- Murphy A. J. and Spray J. G. 2002. Geology, mineralization, and emplacement of the Whistle-Parkin Offset Dike, Sudbury. *Economic Geology* 97:1399–1418.
- Offield T. W. and Pohn H. A. 1977. Deformation at the Decaturville impact structure, Missouri. In *Impact and explosion cratering*, edited by Roddy D. J., Pepin R. O., and Merrill R. B. New York: Pergamon Press. pp. 321–341.
- Offield T. W. and Pohn H. A. 1979. *Geology of the Decaturville impact structure, Missouri*. United States Geological Survey Professional Paper #1042. Washington, D. C.: U. S. Government Printing Office. 48 p.
- Okulitch A. V. 1991. Geology of the Canadian Archipelago and north Greenland; Fig. 2. In *Geology of the Innuitian Orogen and Arctic Platform of Canada and Greenland, geological survey of Canada, geology of Canada 3*, edited by Trettin H. P. Ottawa: Geological Survey of Canada. pp. 435–458.
- Orphal D. L. 1977. Calculations of explosion cratering—II: Cratering mechanics and phenomenology. In *Impact and explosion cratering*, edited by Roddy D. J., Pepin R. O., and Merrill R. B. New York: Pergamon Press. pp. 907–917.
- Osinski G. R. and Lee P. 2005. Intra-crater sedimentary deposits at the Haughton impact structure, Devon Island, Canadian High Arctic. *Meteoritics & Planetary Science* 40. This issue.
- Osinski G. R. and Spray J. G. 2001. Impact-generated carbonate melts: Evidence from the Haughton Structure, Canada. *Earth and Planetary Science Letters* 194:17–29.
- Osinski G. R. and Spray J. G. 2003. Evidence for the shock melting of sulfates from the Haughton impact structure, Arctic Canada. *Earth and Planetary Science Letters* 215:357–370.
- Osinski G. R., Lee P., Spray J. G., Parnell J., Lim D., Bunch T. E., Cockell C. S., and Glass B. 2005a. Geological overview and cratering model for the Haughton impact structure, Devon Island, Canadian High Arctic. *Meteoritics & Planetary Science* 40. This issue.

- Osinski G. R., Spray J. G., and Lee P. 2005b. Impactites of the Houghton impact structure, Devon Island, Canadian High Arctic. *Meteoritics and Planetary Science* 40. This issue.
- Osinski G. R., Lee P., Parnell J., Spray J. G., and Baron M. 2005c. A case study of impact-induced hydrothermal activity: The Houghton impact structure, Devon Island, Canadian High Arctic. *Meteoritics and Planetary Science* 40. This issue.
- Pohl J., Eckstaller A., and Robertson P. B. 1988. Gravity and magnetic investigations in the Houghton impact structure, Devon Island, Canada. *Meteoritics* 23:235–238.
- Pohl J., Stöffler D., Gall H., and Ernstson K. 1977. The Ries impact crater. In *Impact and explosion cratering*, edited by Roddy D. J., Pepin R. O., and Merrill R. B. New York: Pergamon Press. pp. 343–404.
- Redeker H. J. and Stöffler D. 1988. The allochthonous polymict breccia layer of the Houghton impact crater, Devon Island, Canada. *Meteoritics* 23:185–196.
- Robertson P. B. and Sweeney J. F. 1983. Houghton impact structure: structural and morphological aspects. *Canadian Journal of Earth Sciences* 20:1134–1151.
- Roddy D. J. and Davis L. K. 1977. Shatter cones formed in large-scale experimental explosion craters. In *Impact and explosion cratering*, edited by Roddy D. J., Pepin R. O., and Merrill R. B. New York: Pergamon Press. pp. 715–750.
- Schultz P. H., Orphal D. L., Miller B., Borden W. F., and Larson S. A. 1981. Multi-ring basin formation: Possible clues from impact cratering calculations. In *Proceedings of the Conference on Multi-ring Basins: Formation and Evolution*, edited by Schultz P. H. and Merrill R. B. New York: Pergamon Press. pp. 181–196.
- Scott D. and Hajnal Z. 1988. Seismic signature of the Houghton structure. *Meteoritics* 23:239–247.
- Sharpton V. L. 1999. The nature of central peak rings: Evidence from the Houghton Crater (abstract). *Meteoritics & Planetary Science* 34:A107.
- Sharpton V. L. and Dressler B. O. 2003. Excavation flow and central peak rings: Is there a connection? (abstract) LPI Contribution 1155:65–66.
- Sharpton V. L., Dressler B. O., and Sharpton T. J. 1998. Mapping the Houghton impact crater, Devon Island, NWT: Implications for the shape and size of the excavation cavity (abstract #1867). 29th Lunar and Planetary Science Conference. CD-ROM.
- Sherlock S., Kelley S. P., Parnell J., Green P., Lee P., Osinski G. R., and Cockell C. S. 2005. Re-evaluating the age of the Houghton impact event. *Meteoritics & Planetary Science* 40. This issue.
- Shoemaker E. M. and Kieffer S. W. 1974. *Guidebook to the geology of Meteor Crater, Arizona*. Tempe, Arizona: Center for Meteorite Studies, Arizona State University. 66 p.
- Spray J. G. 1997. Superfaults. *Geology* 25:579–582.
- Spray J. G., Butler H. R., and Thompson L. M. 2004. Tectonic influences on the morphometry of the Sudbury impact structure: Implications for terrestrial cratering and modeling. *Meteoritics & Planetary Science* 39:287–301.
- Stewart J. H. 1972. Basin and range structure: A system of horsts and grabens produced by deep-seated extension. *Geological Society of America Bulletin* 82:1019–1044.
- Stöffler D., Gault D. E., Wedekind J., and Polkowski G. 1975. Experimental hypervelocity impact into quartz sand: Distribution and shock metamorphism of ejecta. *Journal of Geophysical Research* 80:4062–4077.
- Thorsteinsson R. and Mayr U. 1987a. The sedimentary rocks of Devon Island, Canadian Arctic Archipelago, Geological Survey of Canada Memoir #411. Ottawa: Geological Survey of Canada. 182 p.
- Thorsteinsson R. and Mayr U. 1987b. Geology of Bear West and Baillie-Hamilton Island, District of Franklin, Northwest Territories. Geological Survey of Canada Map #1614A. Scale 1:250,000.
- Wernicke B. and Burchfield B. C. 1982. Modes of extension tectonics. *Journal of Structural Geology* 4:105–115.
- Wieland F., Gibson R. L., Reimold W. U., and Lana C. 2003. Structural evolution of the central uplift of the Vredefort impact structure, South Africa (abstract). *Meteoritics & Planetary Science* 38:A21.
- Wilshire H. G., Offield T. W., Howard K. A., and Cummings D. 1972. Geology of the Sierra Madera Cryptoexplosion Structure, Pecos County, Texas. USGS Professional Paper #599-H. Washington, D. C.: U.S. Government Printing Office. 42 p.
- Wilson C. W. and Stearns R. G. 1968. Geology of the Wells Creek Structure, Tennessee. State of Tennessee Department of Conservation Division of Geology Bulletin #68. Nashville, Tennessee: State of Tennessee Department of Conservation Division of Geology. 236 p.
- Wittmann T., Kenkmann T., Schmitt R. T., and Stöffler D. 2003. Clastic polymict dikes in the “megablock” sequence of the ICDP-Chicxulub drill core YAX-1 (abstract #1386). 34th Lunar and Planetary Science. CD-ROM.